Nucleic Acids Research, 2023, 1–17
https://doi.org/10.1093/nar/gkad827
RNA and RNA-protein complexes

OXFORD

Dynamics of ribosome composition and ribosomal protein phosphorylation in immune signaling in *Arabidopsis thaliana*

Anna Siodmak[1,†], Federico Martinez-Seidel[2,3,†], Naganand Rayapuram[1,†], Jeremie Bazin[4], Hanna Alhoraibi[5], Dione Gentry-Torfer[2,3], Naheed Tabassum[1], Arsheed H. Sheikh[1], José Kenyi González Kise[1], Ikram Blilou[1], Martin Crespi[4], Joachim Kopka[2] and Heribert Hirt[1,6,*]

[1]Center for Desert Agriculture, Division of Biological and Environmental Sciences and Engineering, King Abdullah University of Science and Technology, Thuwal 23955-6900, Saudi Arabia
[2]Willmitzer Department, Max Planck-Institute of Molecular Plant Physiology, Potsdam, Germany
[3]School of Biosciences, The University of Melbourne, Parkville, VIC, Australia
[4]CNRS, INRA, Institute of Plant Sciences Paris-Saclay IPS2, Univ Paris Sud, Univ Evry, Univ Paris-Diderot, Sorbonne Paris-Cite, Universite Paris-Saclay, Orsay, France
[5]Department of Biochemistry, Faculty of Science, King Abdulaziz University, 21551 Jeddah, Saudi Arabia.
[6]Max F. Perutz Laboratories, University of Vienna, Dr. Bohrgasse 9, 1030 Vienna, Austria

[*]To whom correspondence should be addressed. Tel: +96 6128082959; Fax: +96 6128082959; Email: heribert.hirt@kaust.edu.sa
[†]The authors wish it to be known that, in their opinion, the first two authors should be regarded as Joint First Authors.

Abstract

In plants, the detection of microbe-associated molecular patterns (MAMPs) induces primary innate immunity by the activation of mitogen-activated protein kinases (MAPKs). We show here that the MAMP-activated MAPK MPK6 not only modulates defense through transcriptional regulation but also via the ribosomal protein translation machinery. To understand the effects of MPK6 on ribosomes and their constituent ribosomal proteins (RPs), polysomes, monosomes and the phosphorylation status of the RPs, MAMP-treated WT and *mpk6* mutant plants were analysed. MAMP-activation induced rapid changes in RP composition of monosomes, polysomes and in the 60S ribosomal subunit in an MPK6-specific manner. Phosphoproteome analysis showed that MAMP-activation of MPK6 regulates the phosphorylation status of the P-stalk ribosomal proteins by phosphorylation of RPP0 and the concomitant dephosphorylation of RPP1 and RPP2. These events coincide with a significant decrease in the abundance of ribosome-bound RPP0s, RPP1s and RPP3s in polysomes. The P-stalk is essential in regulating protein translation by recruiting elongation factors. Accordingly, we found that RPP0C mutant plants are compromised in basal resistance to *Pseudomonas syringae* infection. These data suggest that MAMP-induced defense also involves MPK6-induced regulation of P-stalk proteins, highlighting a new role of ribosomal regulation in plant innate immunity.

Graphical abstract

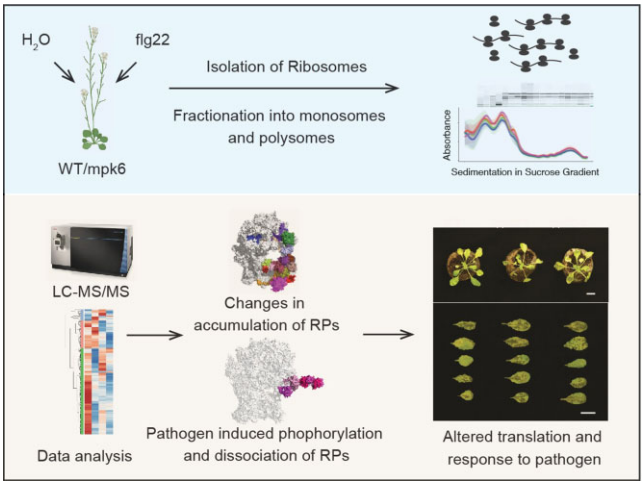

Received: June 24, 2023. **Revised:** September 14, 2023. **Editorial Decision:** September 19, 2023. **Accepted:** September 20, 2023

Introduction

Ribosomes are the motors of translation, which is the conversion of genetic information from mRNA into peptides or proteins (1,2). The eukaryotic 80S cytosolic ribosome is formed by two subunits, the small (SSU-40S) and large (LSU-60S) ribosomal subunits which are composed of rRNA and ribosomal proteins (RPs). The internal constitution and size of ribosomes varies between different eukaryote phyla, with ribosomes of human, rat and yeast being amongst the most studied. Plant ribosomes harbor four different rRNAs (3) and >80 RPs (1,2). Within the ribosomal complex, RPs regulate many processes including monitoring of rRNA assembly and folding and are directly related to the competence of the ribozyme catalytic function (2,4,5). In addition to their ribosome bound functions, RPs can also act as extra-ribosomal components (6,7).

In plants, the diversity of ribosomal heterogeneity is assumed to play an important role in translational regulation (7–12). Ribosomes can differ in terms of rRNA sequence, posttranscriptional modifications, ribosome-associated factors (RAFs) as well as structural RPs and their posttranslational modifications. RAFs are molecules that can attach to the ribosome complexes and affect the translation process as well as ribosome biogenesis (13,14). Structural RPs in their ribosome-bound form can change quantitatively and qualitatively during development (15). For instance, *Dictyostelium discodeum* displays unique RPs within amoebae and sporophytic stages (16,17). Similarly, in etiolated barley leaves, RPs change their association with cytoplasmic ribosomes during greening (18). An additional layer of complexity is found in plants due to genome duplication events, where each RP can be encoded by 2–7 paralogous genes (1). These paralogs can have an identical sequence, however a great number exhibit sequence variations that might be related to specialized functions (19,20). In *Brassica napus* more than half of the RPs have paralogs with opposite expression patterns (21). This evidence suggests that the presence and functions of RPs or their paralogs within a ribosomal complex influence translation. Accordingly, the loss or mutation of several RPs in humans lead to morphological abnormalities, such as cancer or Diamond-Blackfan anaemia (22,23). Similarly, in plants, ribosomal loss-of-function mutations can be embryonic lethal or cause developmental malfunctions (24,25). Such developmental defects, for example, were observed in RPL24B mutants in which vascular patterning and gynoecium structure were perturbated as a result of low expression of auxin response genes (26). Deletion of certain RPs or their paralogs is not necessarily detrimental to translation (27). Briggs & Dinman highlighted one of the misconceptions about the detrimental effect of a below average ribosomal constitution in the fidelity of the translation process. Instead, it was proposed that subtraction of RPs is a realistic means of achieving ribosome specialization. For instance, siRNA of RPL10 (uL1) identified two IRES elements that become less translated in the absence of the RP (27). Similarly, RPL30 (eL30) is necessary to efficiently insert selenocysteine residues into peptide sequences (28). Thus, subtractional heterogeneity is likely to occur as a control mechanism enabling targeted translation.

Ribosomes can differ also in terms of the post-translational modifications of RPs or RAFs. In general, post-translational modifications (PTMs) broaden the range of available amino acids for protein structure changes increasing their variety and function (8). Particularly interesting are reversible modifications which enable cellular signaling (29). An important PTM that has a regulatory effect on translation is phosphorylation. RP phosphorylation status depends on the organ type, developmental stage as well as environmental factors (30–38). In maize, beyond quantitative RP changes, ribosomes are major targets of phosphorylation and specific plant RPs are dephosphorylated upon hypoxia-induced stress (39). In contrast, RPS6 is phosphorylated in response to pathogen infection (40) and this event is known to alter the levels of specific target mRNAs (41). However, the mechanistic relation between pathogen attack and RP-PTM is poorly understood.

Several studies highlight the importance of ribosome compositional changes during biotic and abiotic stresses. In general, these compositional changes reflect RPs that become substoichiometric in ribosomal populations upon specific cues, contrary to the mainstream view of each ribosome having only one copy of all RPs. The major abiotic factors that induce varied RP dynamics are sucrose starvation, hypoxia and cold stress exhibiting conserved specific RP changes within the ribosomal complex (42–47). Similarly, the function of RPs in biotic stress such as pathogen induced plant defense is well documented. The ribosomal proteins RPL12 and RPL19, for example, have been studied in relation to non-host disease resistance (48). Reduced disease resistance was observed in a non-redundant manner in *RPL12* or *RPL19* silenced *Nicotiana benthamiana* and *A. thaliana* (48). The role that ribosomes play during stress regulation is characterized by changes in ribosomal composition. In addition, targeted translation during stress acts as a mechanism to adjust the necessary protein production to specific conditions and it is highly probable that these events are interdependent.

Amongst biotic stresses bacterial infections pose a severe threat for human food safety (49,50). Plants can recognize bacterial flagella to trigger the plant immune system, and this mechanism is called microbe-associated molecular pattern (MAMP)-triggered immunity (MTI) (51). Upon perception of flg22, a peptide of the bacterial flagellin, MAPKs are phosphorylated in order to be activated (52,53). Upon activation, MPK3, MPK4 and MPK6 interact with cytosolic or nuclear substrates such as transcription factors (54) thereby transmitting the stress signals and regulating the stress responses. A link of MPK6 to phosphorylation of RPs was previously suggested by a protein microarray-based search for putative MPK6 substrates (55). In addition, changes in RPs abundance were also reported in a proteomic study of *mpk6* mutants, including the accumulation of ribosomal protein P0 of the P-acidic ribosomal stalk (56). Recently, we showed that the phosphorylation of several RPs changes in *A. thaliana* upon flg22 treatment. In addition, we observed that the phosphorylation status of these RPs was strongly influenced by MPK6 (57). These data suggest a role of MPK6 in translation via ribosomal regulation, but the details of this mechanism so far are unknown.

This study aims to investigate how the bacterial stress response is regulated in plants at the translational level via the function of MPK6. To test this, we treated *A. thaliana* WT and *mpk6* mutant plants with the bacterial MAMP flg22 in order to induce a typical MTI response, and then isolated monosomes and translating polysomes. Our results revealed that ribosomal complexes undergo rapid compositional changes after 1-hour of the flg22 treatment. The ribosome-bound abundances of RPs changed in monosome and polysome enriched

fractions. Moreover, RPs featuring abundance changes were spatially confined to specific regions of the ribosomal complex. First, flg22-induced changes were localized to a specific region of the 40S ribosomal subunit. Second, *mpk6*-specific stress-induced changes were spatially constrained to a region of the 60S subunit. Remarkably, we identified specific changes in the phosphorylation status of the P-stalk protein components. The P-stalk is composed of acidic ribosomal proteins, so-called P-proteins and is involved in the translocation step of the elongation cycle during the protein translation mechanism (58). The eukaryotic P-stalk consists of one P0 protein directly interacting with the 5.8S rRNA, thereby establishing the base of the structure, and P1 and P2, which are attached in the form of dimers to the base forming a protrusion (59–62). The P-proteins have important functions within the ribosomal complex such as promotion of eEF2-dependent GTPase activity (63–67), eEF1 binding (68), and poly(U)-directed phenylalanine synthesis (64,69). The differential regulation of several P-stalk proteins suggests a role of these acidic RP paralogs in the defense regulation of translation. In our work, the observed changes in the phosphorylation status of the P-stalk proteins coincided with their dissociation and thus might explain the strong reduction in bulk translation upon stress perception in plants. Consequently, T-DNA mutants of Arabidopsis deficient in one of the P-stalk components showed increased susceptibility to bacterial infection validating that this ribosomal protein plays a key role in immunity. Overall, our results give new insight into the regulatory mechanisms governing translational control in the immune response.

Materials and methods

Plant material and culture conditions

For phosphoproteomic experiments, Arabidopsis thaliana ecotype Columbia-0 (Col-0) was used as wild-type (WT) plant. The *mpk6–2* mutant (SALK_073907) (70) was generated in *Arabidopsis thaliana* ecotype Col-0. The RPP0C locus, isolation of the *rpp0c* mutant and verification of the T-DNA mutant by sequencing of the respective PCR fragment is shown in Figure S2. Plants were grown, treated and harvested as described in (53). Three biological repeats were prepared for mpk6 mutant plants and from WT plants. Within each biological repeat, one sample was treated for 15 min with water and another sample for the same duration with 1 μm flg22 (final concentration).

For polysome isolation *Arabidopsis thaliana* ecotype Columbia-0 (Col-0), and *mpk6-2* (SALK_073907) seeds were stratified at 4°C for 48 hours and were grown under long day conditions (16 h light, 8 h darkness) in Percival growth chambers for 16 days at 23°C and 60% humidity on MS media.

Monosome and polysome isolation coupled to MS

Ribosomal protein fractions were obtained as described by (71). Sixteen days old Arabidopsis seedlings were treated for 1 h with 1 μM flg22 or H_2O. The seedlings were immediately frozen under liquid nitrogen. Plant polysomes were isolated following the instructions by Mustroph, Juntawong, and Bailey-Serres (71) with some modifications. Namely, sucrose gradients with separated ribosome complexes were monitored after ultracentrifugation by collecting approximately 250 μl fractions at a flow rate of 0.75 ml min-1 with continuous absorbance measurement at $\lambda = 254$ nm to monitor rRNA absorbances using a Brandel BR-188 density gradient fractionation system (Alpha Biotech Ltd, Glasgow, UK). This procedure was repeated in biological triplicates for each of our experimental conditions. RNA was extracted and analyzed using an Agilent 2100 Bioanalyzer and an RNA 6000 pico kit according to the manufacturer's instructions (Agilent Technologies, Santa Clara, CA, USA) as previously described in Firmino *et al.* (2020). The microfluidic UV traces were scaled to a single sample to assess the rRNA composition of each fraction, and the process allowed the nature of each of the fractions to be fully elucidated in terms of their ribosomal fraction by analyzing the changes in 25S to 18S rRNA, clearly showing the transitions from 40S to 60S and the stabilization of the ratio around 1.6 in polysome samples. Protein concentrations were measured by DC microplate assay. Then collected polysomal fractions were trypsin digested and analyzed by mass spectrometry.

Phosphoproteomic analysis

The phosphopoteomic analysis was performed as previously described in (57).

Pathogen assay

The virulent strain of *Pseudomonas syringae* pv *tomato* DC3000 (*Pst* DC3000) strain was grown and maintained on a LB agar plates at 28°C. The *Pst* DC3000 growth and inoculation procedure was carried out as described in (72). In brief, 1×10^5 cells/ml were resuspended in 0.1% Silwett L-77 solution and 4 weeks of *A. thaliana* plants were sprayed for 4 s. As a mock inoculation, leaves were sprayed with 0.1% Silwett L-77 solution.

Data analysis and informatics

The acquired MS data were background-subtracted, smoothed and Progenesis QI V2.0 for proteomics (Nonlinear Dynamics; Waters Corporation) was used for automated data processing and database searching. The tool Progenesis QI V2.0 performs multivariate statistics on protein measurements to make confident conclusions and generate a protein-based report of any given experiment. Advanced statistical tools - including ANOVA, power analysis and q-values (for false discovery rate) are utilized to arrive at statistically significant differences. The generated peptide masses were searched against TAIR10 protein database using the Progenesis QI V2.0 for proteomics, for protein identification and quantification.

The comparisons were made between the mean ± standard error of the mean values of the readings of each subset of samples, such as the genotypes and conditions. The data were filtered to show only statistically significant [$P < 0.05$; analysis of variance (ANOVA) and post hoc Tukey's test] changes in protein concentration with maximum fold change (MFC) ≥1.5.

Protein annotation

Search parameters in Mascot were as follows: database TAIR10; enzymatic specificity; tryptic with two fragmented ions. FDR was set to 1% for both peptide-spectrum matches and proteins. Relative quantification was carried out using the Progenesis software. Proteins were precipitated and then proteolyzed with trypsin and phosphopeptides were enriched

using the IMAC resin as described in (53). Each comparison distinguished proteins with significantly changing abundance (i.e. the proportion of proteins with decreasing or increasing abundance during different conditions and in each mutant, respectively).

Gene ontology (GO)

AgriGO website was used for gene ontology analysis.

Ribosomal protein dynamics

Ribosomal proteins were named according to both the old and new nomenclature as proposed previously (73) in order to cover any ambiguity across different naming schemes for ribosomal proteins.

Normalization of protein abundances

Normalization was performed using Progenesis software. As an alternative normalization, ribosomal protein abundances were treated as previously described with minor modifications (47). In brief, a normalization factor was built separately for 40S and 60S subunit proteins by summing their abundances in individual samples. In this way, data was normalized to the recovered amounts of ribosomal complexes in each separate fraction.

Normalized matrices featuring the abundances of ribosomal proteins across biological treatments were used for the subsequent analyses.

Ribosome accumulation

Ribosome accumulation measurement was performed analyzing A260 absorption levels of sucrose fractions. Each of the resulting ribosomal fractions was further analyzed using the Bioanalyzer pico RNA assay according to the manufacturer's instructions and after RNA extraction with TRIZol as previously described (74). This allowed determination of the 25S to 18S rRNA ratio of each fraction and thus identification of the position of the free and translating ribosomes.

Protein abundances class comparison

Mean comparisons of protein abundances across treatments was performed using an ANOVA univariate statistical test followed by the post-hoc Tukey HSD correction. The significant P adjusted values were then used to determine if specific treatments caused a significant decrease or increase in protein accumulation.

Spatial analysis

The spatial analyses of ribosomal proteins within the ribosomal complex made use of the best resolved plant cytosolic ribosome structure to date (75). The wheat 80S monosome structure with PDB entry code 4V7E was used to explore the spatial localization of significant changes and to test if those changes were significantly constrained to parts of the complex as detailed in the python algorithm $COSNet_i$ (76). The details of its usage can be found in a GitHub repository (https://github.com/MSeidelFed/COSNet_i).

Results

Flg22-induced changes in phosphorylation of ribosomal proteins

In a previous phosphoproteomic approach, WT and *mpk3*, *mpk4* and *mpk6* mutant plants were mock- or flg22-treated for 15 min (57). Cytoplasmic phosphopeptide enrichment by IMAC and LC-MS/MS based quantification identified a number of RPs to be differentially phosphorylated in response to MAMP signaling (Figure 1 A-D). Importantly, many of these MAMP-induced RP phosphorylation events were compromised in *mpk6* mutant plants but only to a lesser degree or not at all in *mpk3* and *mpk4* mutant plants, respectively, indicating a specific function of MPK6 in the phosphorylation of RPs during MAMP signaling. Analysis of these RP phosphopeptides showed an acidic consensus sequence around the S/T phosphorylation site which does not conform to the S/TP minimal requirement for MAPK targets. We therefore conclude that MAMP-triggered MPK6 regulates a downstream protein kinase that is responsible for phosphorylating this set of RPs.

Flg22-induced changes in ribosomal complexes and proteins

These results prompted us to further investigate the role of MPK6 in altering the dynamics and composition of ribosomal complexes in defense signaling. To understand the possible correlation between RPs from translating and non-translating ribosomes, we investigated monosomal and polysomal fractions from WT and *mpk6* plants upon mock and flg22 treatment. After 1 h of flg22 or mock (control) treatment, RPs were purified and subsequently analyzed by LC–MS/MS mass spectrometry (Figure 2A). Three biological replicates of WT as well as *mpk6* mutant lines were analyzed under flg22 and control conditions. In this way, the accumulation and protein composition of monosomes and polysomes and their RP-PTM landscape were quantified (Figure 2A). (Supplementary Tables 1 and 2).

UV_{254nm} absorption spectra and RNA analysis of the purified ribosomal fractions showed a trend towards depletion of monosomes and accumulation of free ribosomal subunits in WT plants upon treatment with flg22 (Figure 2B). *mpk6* mutants already showed a trend towards intrinsic depletion of monosomes in the absence of treatment, indicating that MPK6 may play an important role in altering ribosome accumulation dynamics. This conclusion was further supported in analyzing the MAMP-induced changes in the ribosomal profiles, showing opposite trends in WT and *mpk6* mutant plants upon flg22 treatment (Figure 2B).

We also annotated the RP families and their specific paralogs, including the relative abundances across samples and experimental conditions. These results indicate that the ribosomal proteome changes significantly upon flg22 treatment and that a part of these changes are MPK6 dependent.

Next, we compared monosomal and polysomal protein compositions in WT and *mpk6* plants in response to flg22 treatment (Supplementary Figure S1A, Table S1). The MS data analysis revealed that no specific RPs accumulated exclusively in WT or *mpk6* under either mock (H_2O) or flg22 treated conditions. Therefore, we quantified the relative abundances of the polysomal and monosomal proteins in the different samples. Comparing the polysome proteomes of mock and flg22 treated WT and *mpk6* plants, we identified a to-

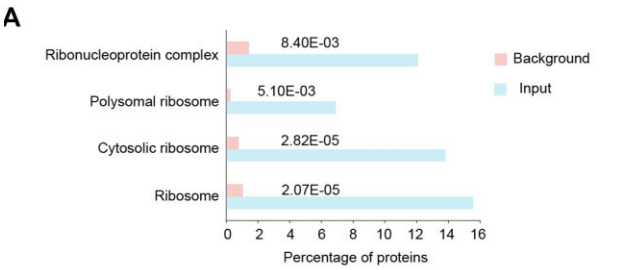

B

Term ID	Term Description	% Input	% Background	FDR
GO:1990904	Ribonucleoprotein complex	11.48	1.35	8.40E-03
GO:0042788	Polysomal ribosome	6.56	0.25	5.10E-03
GO:0022626	Cytosolic ribosome	13.11	0.74	2.82E-05
GO:0005840	Ribosome	14.75	0.98	2.07E-05

C

AGI	Protein Description	Function
AT2G27720	P2z (RPP2A)	60S acidic ribosomal protein P2-1
AT5G13850	NACA3	targets ribosome-nascent polypeptide complexes
AT5G47700	P1y (RPP1C)	60S acidic ribosomal protein P1-3
AT1G01100	P1w (RPP1A)	60S acidic ribosomal protein P1-1
AT2G27710	P2y (RPP2B)	60S acidic ribosomal protein P2-2
AT3G12390	NAC	targets ribosome-nascent polypeptide complexes
AT3G11250	uL10x (RPP0C)	60S acidic ribosomal protein P0-3
AT3G44590	P2w (RPP2D)	60S acidic ribosomal protein P2-4
AT3G49010	eL13z (RPL13B - BBC1)	60S ribosomal protein L13-1 (BBC1 homolog)
AT3G44750	HDA3	Histone deacetylation
AT4G32720	La1	RNA binding activity
AT4G38130	HD1	Histone deacetylase
AT1G17745	PGDH	Serine biosynthesis
AT2G21470	SAE2	Ubiquitin-activating enzyme
AT1G15750	TPL	Transcriptional repressor
AT1G66680	AR401	Methyltransferase
AT3G03570	Protein of unknown funciton	Signal transduction

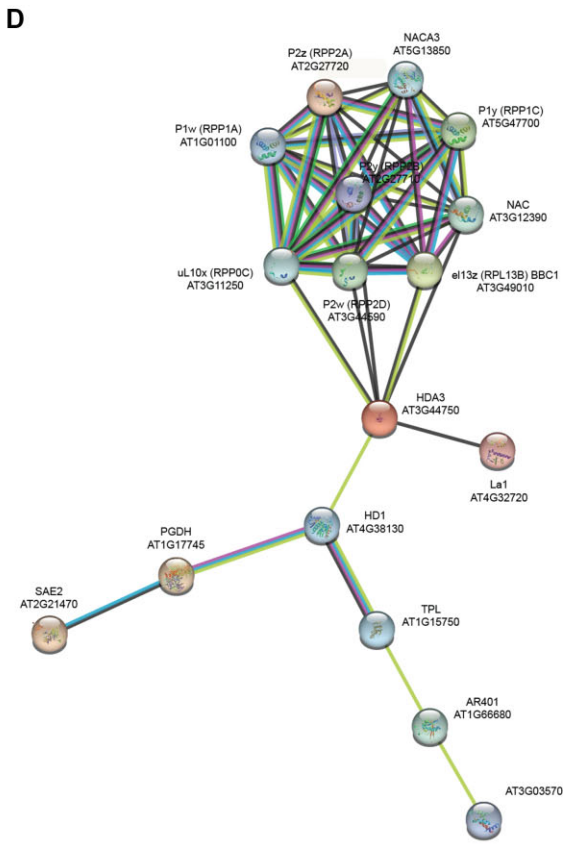

Figure 1. Protein interaction network and GO enrichment. (**A**) GO enrichment analysis of the MPK6-dependent phosphoproteins showed enrichment of proteins associated with ribosomes, cytosolic ribosomes, polysomal ribosomes and ribonucleoprotein complex. (**B**) Table showing the GO term IDs, the term descriptions, percent enrichment in the input, the background and the associated false discovery rate (FRD). (**C**) All phosphoproteins whose phosphorylation changed in response to flg22 treatment in an MPK6-dependent manner. (**D**) MPK6-regulated phosphoproteins of C were used to generate a network using STRING (version 11.5). Data are from three independent biological replicates.

tal of 510 differentially accumulating proteins with 239 reduced and 271 enhanced protein abundance (Figure 3A). In WT, a total of 159 proteins were differentially expressed upon flg22 treatment (60 down- and 99 up-regulated). Importantly, the comparison of WT-flg22 versus *mpk6*-flg22 proteomes revealed a total of 212 differentially abundant proteins (163 enhanced and 49 reduced) (Figure 3A). We generated boxplots of the quotient or ratio of the sum of all 40S and all 60S RP abundances per experimental sample (Figure 3C). Fluctuations in this ratio reflect RP substoichiometry across experimental samples. Together with the heatmap analysis (Figure 3B) and the 40S/60S ratios (Figure 3C) these results show that flg22 signaling strongly influences the ribosomal proteome composition and furthermore that MPK6 plays a major role in this process. GO term analysis of the clusters in the heat map resulted in almost identical GO terms of ribosome biogenesis, translation, and gene expression (Supplementary Tables 3 and 4). These results are not surprising given the fact that the analyzed fractions are purified ribosomal complexes. We then clustered the proteins for cytoplasmic and organellar RPs separately (Figure 3D and E, respectively). Interestingly, flg22 treatment of WT plants mostly resulted in enhanced abundance of cytoplasmic RPs (Figure 3D) but reduced abundance of organellar RPs (Figure 3E). Untreated mutants of *mpk6* did not vary strongly from untreated WT but strongly compromised the changes observed in flg22-treated WT plants (Figure 3D and E). These results confirm that flg22 signaling strongly affects ribosomal composition in WT and that MPK6 affects only the abundance of particular subset of these RPs.

We also noted that a number of RPs of either mitochondrial or plastid origin were differentially regulated in their abundance. To clarify the impact of immune signaling on organellar ribosome organization, we therefore generated a heat map of the flg22-induced ratios of differentially abundant cytosolic, mitochondrial and plastid RPs from WT and *mpk6* (Figure 3F). Overall, we observed that flg22 signaling affects different RPs in a complex manner and that MPK6 has the strongest differential effect on the regulation of the mitochondrial and plastid ribosomal complexes.

We also assessed whether polysome and monosome proteome composition varies significantly upon flg22 treatment. For this purpose, we analyzed the monosome proteomes of flg22- and mock-treated WT and *mpk6* plants (Figure 4). We observed a total of 173 differentially abundant proteins under all four conditions, with 76 of them showing an flg22-dependent regulation in WT plants. The comparison of WT-flg22 versus *mpk6*-flg22 monosome proteomes revealed 62 differentially abundant proteins (with 40 enhanced and 22 reduced abundance) which showed a visible different pattern by heat map (Figure 4B) and 40S/60S ratio (Figure 4C) analysis. We then again separated the cytoplasmic (Figure 4D) from the organellar RPs (Figure 4E). Opposite to the situation of polysomes (Figure 3D), where flg22-induced enhancement of cytoplasmic RPs, monosome cytoplasmic RP levels mostly de-

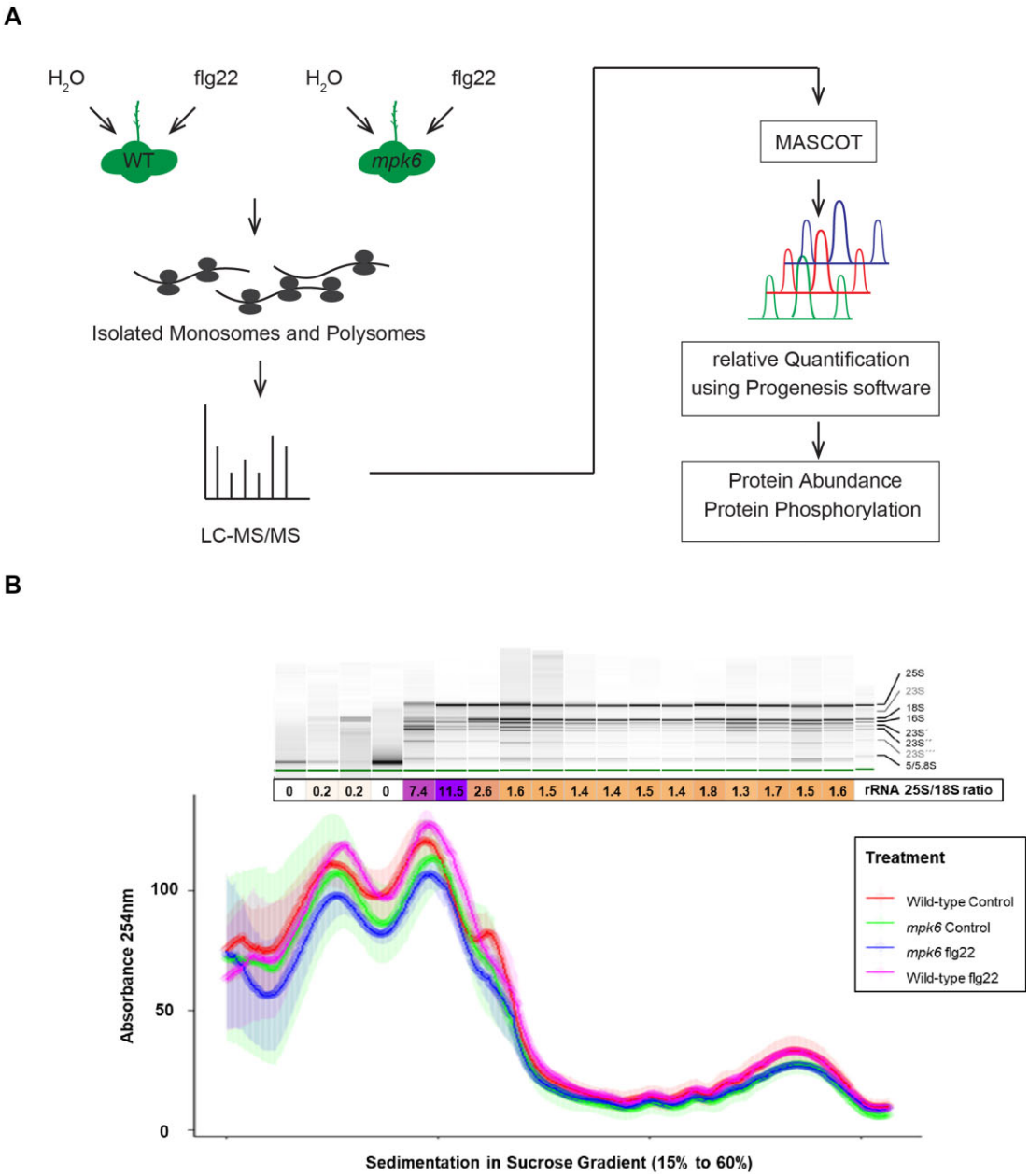

Figure 2. Workflow and accumulation dynamics of ribosomes and their constituent proteins of *mpk6* and WT ribosomal complexes. (**A**) Flowchart of experimental setup. (**B**) Representative profiles of isolated ribosomal complexes purified from *mpk6* and WT. Each experimental condition represents the mean of three biological replicates ($n = 3$) with their respective standard deviation outlined as error bars. The area under the curve of the peak was integrated and pairwise statistical comparisons were made using ANOVA + Tukey HSD (Supplemental File S3A–G). No *P* values were found to be <0.05. The largest ribosomal complexes correspond to polysomes with a high degree of oligomerization to sediment further into sucrose gradients, with the ratio of 25S to 18S rRNA close to 1.6 reflecting the relative abundances of 40S to 60S subunits in fully assembled and translationally competent polysomes and outlining the purity of the fractions obtained from sucrose gradient separation and fractionation. Data are from three independent biological replicates.

creased abundance upon flg22 treatment (Figure 4D). A similar opposing regulation was observed for organellar RPs in flg22 treated WT plants. These data imply that RP abundance in different compartments is tightly choreographed during immune signaling.

Flg22-triggered signaling induced changes in polysome composition

One of our main objectives was to determine whether MAMP-signaling induces compositional changes in ribosomes which might be linked to flg22-induced translational modulation. We therefore focused on the 510 proteins that were identified from the actively translating polysome fractions (Figure 3A). RPs changing their abundance in polysomal complexes upon flg22 treatment were assumed to play a role in defense response. Using these criteria, we found numerous RPs that showed significant differential regulation upon flg22 treatment. For example, RPS19C/eS19 (AT5G61170), RPP1A (AT1G01100), RPS7A/eS7 (AT1G48830), RPP3A (AT4G25890), RPS19A/eS19 (AT3G02080) show

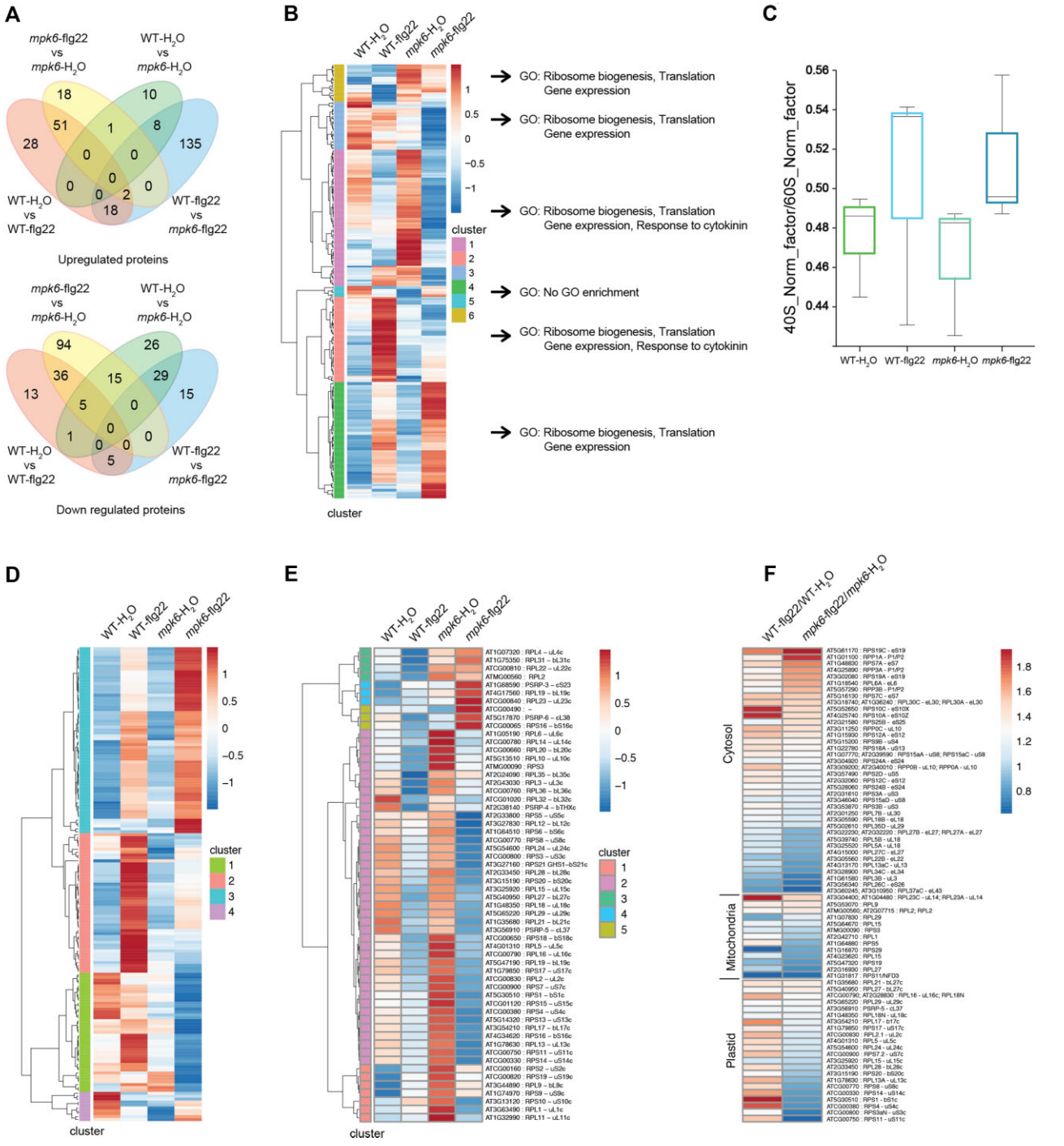

Figure 3. Proteome analyses in polysome fraction of WT-H_2O, WT-flg22, *mpk6*-H_2O and *mpk6*-flg22. (**A**) Venn diagrams showing unique and overlapping proteins with reduced and enhanced abundance in the different samples and treatments. (**B**) A heatmap showing varying abundances of all the proteins identified from the polysome fraction and the GO term enrichments for each of the clusters. (**C**) Boxplots outlining the quotient or ratio between the sum of all 40S RP abundances and the sum of all 60S RPs abundances per experimental sample, fluctuations in this ratio reflect global RP substoichiometry as it relates to 60S to 40S subunit abundances across experimental samples. (**D**) A heatmap of a subset of proteins from the entire data set that correspond to all the translation initiation factors, ribosome biogenesis factors as well as the mitochondrial and chloroplastidic ribosomal proteins. (**E**) A heat map of only the annotated ribosomal proteins of Arabidopsis and their paralogs. (**F**) Heatmap of the abundance ratios of cytosolic, mitochondrial and plastid RPs in WT and *mpk6* with and without flg22 treatment. The red color in the range indicator represents higher amounts and blue color represents a reduction in abundance of the corresponding protein. Data are from three independent biological replicates.

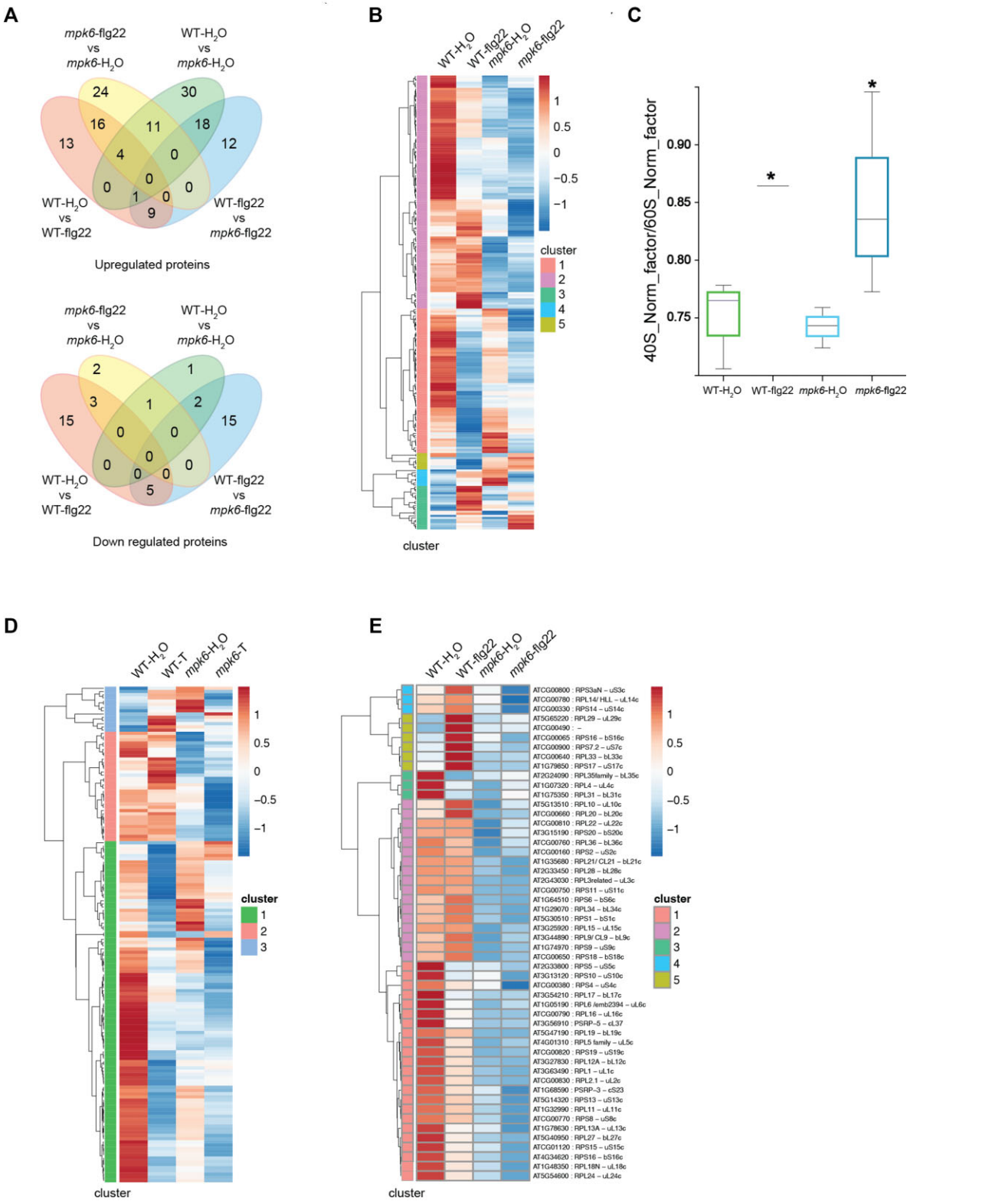

Figure 4. Proteome analyses in monosome fraction of WT-H_2O, WT-flg22, *mpk6*-H_2O and *mpk6*-flg22. (**A**) Venn diagrams showing unique and overlapping down and up regulated proteins in the different samples and treatments. (**B**) A heatmap showing varying abundances of all the proteins identified from the polysome fraction and the GO term enrichments for each of the clusters. (**C**) Boxplots outlining the quotient or ratio between the sum of all 40S RP abundances and the sum of all 60S RPs abundances per experimental sample, fluctuations in this ratio reflect global RP substoichiometry as it relates to 60S to 40S subunit abundances across experimental samples. Asterisks indicate significant differences by t-test at $P \leq 0.05$. The lack of variability in WT – flg 22 treated samples reflects stable ratios between 40S and 60S abundances as compared to the variability observed for the other treatments. (**D**) A heatmap of a subset of proteins from the entire data set that correspond to all the translation initiation factors, ribosome biogenesis factors as well as the mitochondrial and plastid ribosomal proteins. (**E**) A heat map of only the annotated ribosomal proteins of Arabidopsis and their paralogs. Data are from three independent biological replicates.

enhanced, whereas eL22, L13, L34e and RPL3B (AT1G61580) reduced abundance. Many of these flg22-regulated proteins are differentially abundant in *mpk6* mutants, indicating a role of MPK6 in their regulation.

Interestingly, flg22-induced changes were observed in abundance levels for several protein components of the P-stalk ribosomal substructure, namely RPP0B, RPP0C, RPP1A, RPP3A and RPP3B (Figure 3F and 5, Supplementary Figure S1B, Table S2).

In order to better understand the defense response process, we went beyond specific changes of proteins and investigated if substoichiometric RPs, ubiquitously present in all conditions, were significantly localized to specific ribosomal regions after MAMP treatment in WT. Significantly changed or substoichiometric RPs were mapped into a 3D rendering of the plant cytosolic ribosome and spatial dependencies were identified by applying the COSNet$_i$ algorithm (76). Specific regions within the ribosomal complex changed upon flg22 treatment in WT plants (Figure 6B). One region emerged from this analysis was allocated to the 40S subunit adjacent to the mRNA and tRNA entry sites. The structurally coherent region was composed of RPS3/uS3, RPS5/uS7, RPS10/eS10, RPS12/eS12, RPS16/uS9, RPS17/eS17, RPS18/uS13, RPS20/uS10, RPS29/uS14 and RACK1, indicating that significant changes occur in this region as compared to a null hypothesis of random allocation across the complex. Thus, overrepresentation of substoichiometric RPs (i.e. in this specific case RPs that decrease their subunit-bound abundance) in a specific 40S region only in actively translating polysomes, may signal defects or alterations in the process of mRNA or tRNA recruiting. To what extent these regional modifications are preexisting the stimulus or triggered by it remains an open question. However, these rapid changes in RP paralog composition could be crucial for defense signaling. Finally, our results highlight the importance of the fast rearrangement of the 40S subunit in defense, a response that is visible after one hour of the initial MAMP stimulus.

Flg22 signaling induced MPK6-dependent changes in 40S and 60S ribosomal complexes in polysomes

Next, we analyzed changes within proteins isolated from the actively translating ribosome fractions of *mpk6* mutants in order to investigate the role of MPK6 in immune signaling. As done before (76), the COSNet$_i$ algorithm was used in order to annotate and investigate the relative localization of MPK6-dependent RPs upon flg22 induction. *In silico* modeling revealed that flg22-triggered MPK6 signaling induced significant changes within two regions of the ribosome that are expanding to the 40S and 60S subunits. The first region is composed of the previously mentioned RPs identified in the conserved region of flg22-treated WT (except RPS10/eS10 and RPS12/eS12) and in addition RPS14/uS11, RPS19/eS19, RPS25/eS25, RPS26/eS26 and RPS28/eS28. Region 2 was confined to RPS5/uS7, RPL5/uL18, RPL11/uL5, RPL15/uS19, RPL15/eL15, RPS18/uS13, RPS19/eS19, RPL21/eL21, RPS25/eS25 and RPS36/eL42 (see Figure 6C and D). Thus, the main difference to WT was that the equivalent region was less specific and more spread across both subunits in the *mpk6* mutant. Although in both cases the 40S RPs belonging to the significantly sub-stoichiometric region were overlapping whereas RPs of the 60S subunit were *mpk6* specific.

Flg22-induced phosphorylation events in the ribosomal P-stalk

Examination of the phosphoproteome data (57) also revealed that a major reprogramming in regard to phosphorylation events occurred in the P-stalk of the ribosome. In total, 8 P-stalk RP paralogs were identified to change their phosphorylation status upon flg22 treatment of *A. thaliana* plants (Figure 7). In *mpk6* mutants RPP0B (AT3G09200) and RPP0C (AT3G11250) showed increased phosphorylation, while RPP1A (AT1G01100), RPP1C (AT5G47700), BBC1 (AT3G49010), RPP2B (AT2G27710), RPP2A (AT2G27720) and RPP2D (AT3G44590) showed reduced phosphorylation upon flg22 treatment compared to treated WT. Interestingly, while the base protein RPP0 became phosphorylated, the protrusion protein paralogs P1 and P2 of the P-stalk were dephosphorylated upon flg22 treatment, suggesting that MPK6 regulates the phosphorylation dynamics of these P-stalk proteins.

RPP0C is crucial for pathogen resistance

The changes in the abundance and phosphorylation levels of RPs in our study were obtained from MAMP-treated *A. thaliana* plants. RPP0C was selected as the most promising candidate as this protein not only accumulates significantly upon flg22 treatment but was also affected in its phosphorylation status. In order to assess the importance of the P-stalk RPP0C protein in defense, we obtained and verified two independent T-DNA insertion lines of RPP0C (Supplementary Figure S2) and challenged these plant lines with the virulent bacterial pathogen *Pst* DC3000 (Figure 8A–D). Treatment of these two independent knock out and knock down SAIL-lines (Supplementary Figure S2) by spray inoculation with *Pst* DC3000 showed that both *rpp0C* lines were more susceptible to infection by the bacterial pathogen compared to WT. The number of bacteria per leaf disc in *rpp0C-1 and rpp0C-2* plants was elevated by more than 10-fold when compared to WT (Figure 8A and B). These results show that RPP0C function is crucial for the resistance of *Arabidopsis thaliana* towards pathogens such as the bacterial pathogen *Pst* DC3000.

Discussion

MAP Kinases play an important role in plant immunity (77). In our recent phosphoproteomics study, we observed changes in the phosphorylation levels of several ribosomal proteins in *A. thaliana* upon flg22 treatment. We observed that these events were strongly influenced by the activity of the MPK6 kinase (57). These findings are supported by the identification of several ribosomal proteins as MPK6 targets in a protein microarray study (55) and changes in ribosomal protein abundances in *mpk6* mutant plants (56). These results suggest a potential influence of the MAMP-triggered MAPK cascade on translation via ribosomal regulation, but the details of this mechanism were so far unknown. MPK6 is well known to interact with substrates which affect transcriptional regulation but new evidence has emerged showing that MPK6 can also affect substrates that induce post-transcriptional events (78). Examples of such substrates are proteins regulating mRNA decapping, degradation or storage (79–81). Thus, by altering mRNA dynamics, such substrates might bridge the link between an initial stimulus, the activation of the MPK6 cascade and the translation of a defense-related proteome. In this

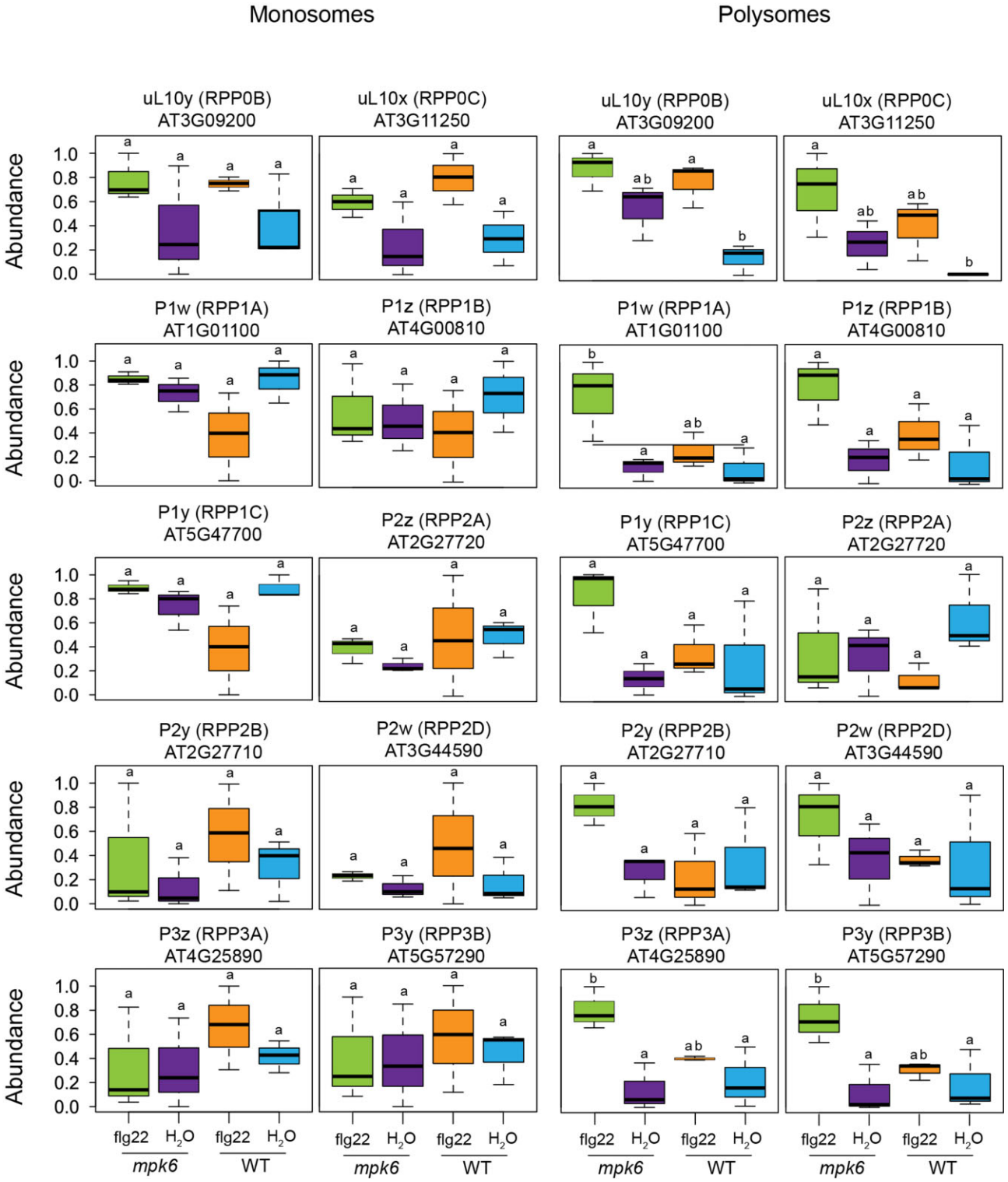

Figure 5. Changes in ribosomal protein abundances of the P-Stalk. Tukey HSD plot of polysomes of flg22 treated and H_2O treated *mpk6* and WT plants. Normalized ribosomal protein abundances were used to compare the means across treatments using an ANOVA followed by a post-hoc Tukey HSD test. The summary graphs are boxplots featuring the main statistics of the protein abundance vectors. Significance is denoted by lack of shared letters between the identifiers on top of two boxes. The comparisons were done across monosomes and polysomes of flg22-treated and untreated *mpk6* and WT plants indicating RPP0B; RPP0C; RPP1A; RPP1B; RPP1C; RPP2A; RPP2B; RPP2D; RPP3A and RPP3B. Data are from three independent biological replicates.

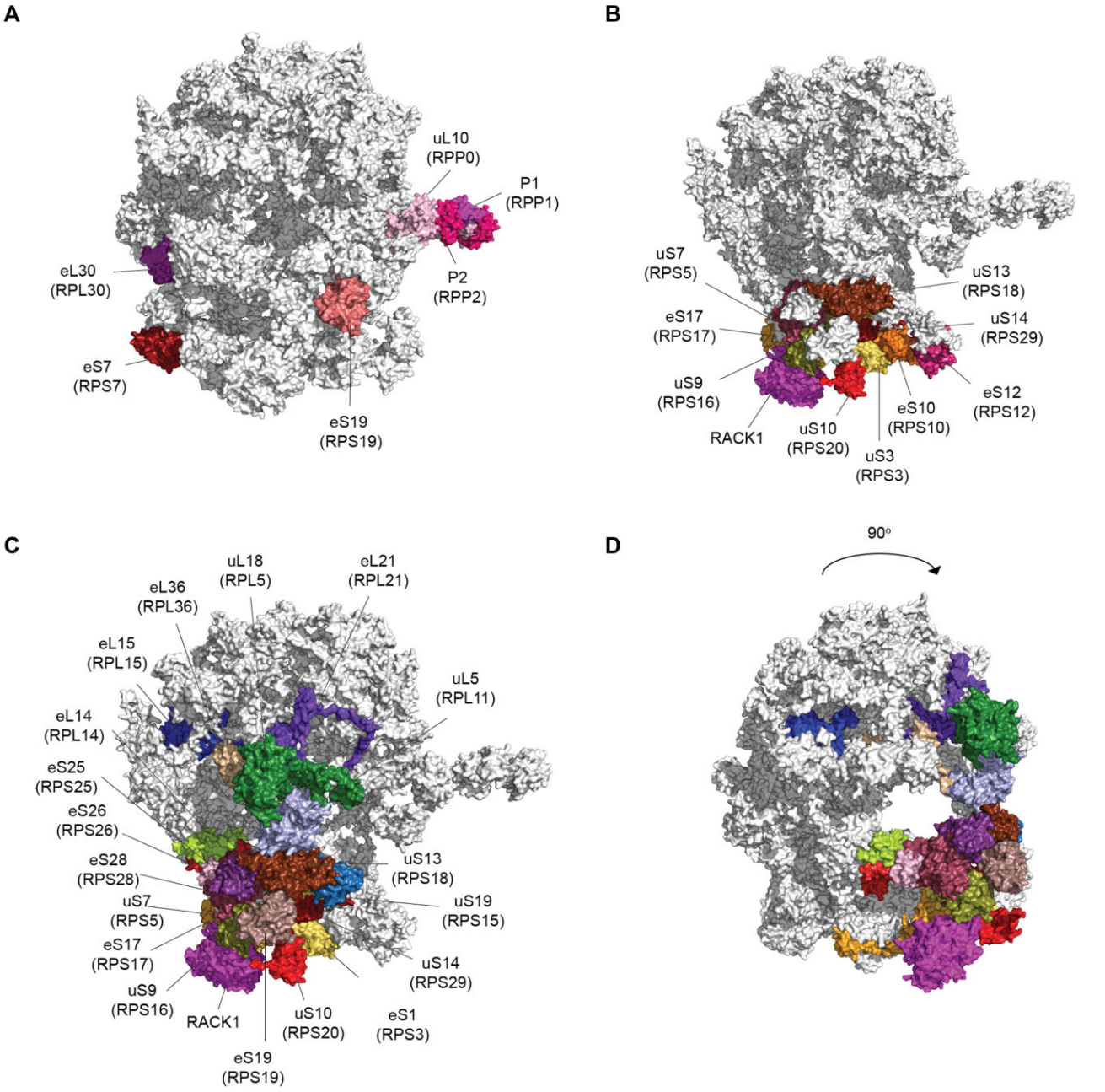

Figure 6. Differential accumulation of RPs in polysomes in response to MAMP signaling. 2D rendering of an originally 3D display of the wheat 80S monosome (75,114) featuring the 60S subunit on top and 40S subunit on bottom. Proteins of interest are highlighted in different colors. Only ribosome proteins are shown and the rRNA backbone is removed for clear display. (**A**) Front view of 40S and 60S. RPs highly affected in abundance changes by flg22 treatment. (**B–D**) Highlighted RPs represent significantly remodelled coherent ribosomal regions as picked up by the COSNet$_l$ (76) methodology that feature higher prevalence of proteins with significant abundance changes as compared to the overall complex. (B) Side view of 40S and 60S. Represents the substoichiometric significant abundance changes in RPs from polysomes of WT flg22-treated as compared to WT H_2O-treated. (C, D) Represents substoichiometric abundance changes in RPs from polysomes of *mpk6* flg22-treated as compared to *mpk6* H_2O-treated.

work, we focused on the interaction between MAP Kinases and the translation machinery to better understand the *in vivo* status of the defense related proteome. Translation regulation has a key function during gene expression, especially during stress (82–87). Moreover, transcript levels only partially reflect protein amounts and well-established scientific methods used to analyze gene expression levels often do not represent the physiological state at the proteome level (88).

Upon recognition of pathogens, plants undergo a vast transcriptional reprograming to inhibit growth and use energy sources for producing defense-related genes (89,90). Defense induced transcriptional reprogramming has been extensively investigated during recent years, but translational reprograming is still poorly understood. Recently, Xu *et al.* (91) reported interesting insight about defense-induced translational changes. Ribosomal footprint sequencing revealed elf18-MAMP specific changes in Arabidopsis. A specific purine-rich motif within actively translated mRNAs was identified and named the 'R-motif'. This inhibitory motif of basal translation was crucial for MAMP-induced translation of defense related

A

AT-number	Name	Phosphosite
AT3G09200	uL10y (RPP0A)	[VEEKEE(s)*DEEDYGGDFGLFDEE]
AT3G11250	uL10x (RPP0C)	[VEEKKEE(s)*DEEDYEGGFGLFDEE] [KEE(s)*DEEDYEGGFGLFDEE]
AT1G01100	P1w (RPP1A)	[KDEPAEE(s)*DGDLGFGLFD] [KKDEPAEE(s)*DGDLGFGLFD]
AT5G47700	P1y (RPP1C)	[KDEPAEE(s)*DGDLGFGLFD] [KKDEPAEE(s)*DGDLGFGLFD]
AT3G49010	eL13z (RPL13B)	[VKAGD(st)*PEELANATQVQGDYLPIVR] [VKAGDS(t)*PEELANATQVQGDYLPIVR] [AGD(s)*TPEELANATQVQGDYLPIVR,AGDS(t)*PEELANATQVQGDYLPIVR] [AGD(st)*PEELANATQVQGDYLPIVR] [AGDS(t)*PEELANATQVQGDYLPIVR]
AT2G27710	P2y (RPP2B)	[KEEKEE(s)*DDDMGFSLFE] [EEKEE(s)*DDDMGFSLFE] [EE(s)*DDDMGFSLFE]
AT2G27720	P2z (RPP2A)	[KEEKEE(s)*DDDMGFSLFE] [EEKEE(s)*DDDMGFSLFE] [EE(s)*DDDMGFSLFE]
AT3G44590	P2w (RPP2D)	[KEEKEE(s)*DDDMGFSLFE] [EEKEE(s)*DDDMGFSLFE] [EE(s)*DDDMGFSLFE]

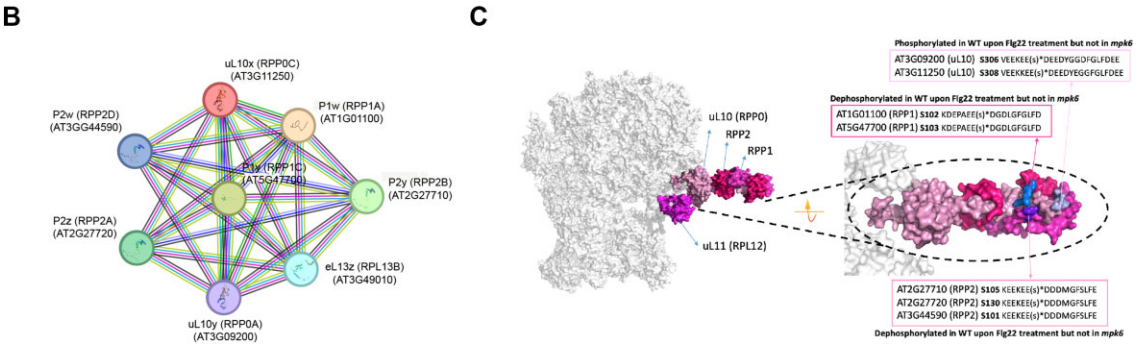

Figure 7. MAMP-induced MPK6-dependent phosphorylation of ribosomal proteins. (**A**) List of flg22-induced MPK6-dependent differentially phosphorylated ribosomal proteins. (**B**) STRING network of differentially phosphorylated RPs. (**C**) Significant region picked up by the algorithm COSNet$_i$ (76) outlining that the differential phosphorylation events that are MPK6 dependent, are also significantly confined to the P-stalk. Thus, colored RPs represent proteins affected in phosphorylation changes in *mpk6* mutants upon flg22 treatment compared to treated WT. Specific terminus near the phosphorylation sites are highlighted for each RP.

mRNA by interaction with poly(A)-binding proteins. Overall, transcription and translation seemed to be very poorly related as mRNA levels did not overlap with actively translated mRNAs. Therefore, the defense related proteome is assumed to emerge as a mixture of transcriptional and translational regulation (91). Similarly, RPS2-mediated effector triggered immunity (ETI) has effects on global translation (92). ETI induced translational changes occur at a later time point compared to MTI-induced changes and in contrast to MTI, ETI showed a good correlation between transcription and translation, indicating a coregulation of both processes. In addition, ETI induced defense did not lead to a downregulation of basal translation and showed an induction of metabolic pathways (92).

To investigate the connection between MPK6 and ribosomes we isolated monosomes and polysomes from WT and *mpk6* plants. MAMP-triggered signaling induced the accumulation of monosomes in *mpk6* mutants. Interestingly, an increased amount of monosomes was also observed under stress in maize (39). In maize, an increase of monosomes and free ribosomal subunits occurred simultaneously with a decrease in polysomes undergoing hypoxia and was reversible when the stress was removed. A simultaneous increase in the synthesis of new ribosomal proteins during stress (39), supports the idea that a rearrangement of ribosomes plays a role in the defense response against pathogen attack.

Our results show that MAMP triggers a strong and rapid ribosomal reorganization (1 hour). MAMP-induced changes in RPs and RAF abundance in ribosomal complexes suggest that these either might get newly synthesized or remodeled, thereby explaining the differential accumulation of RPs and their paralogs. It was proposed that stress in plants induces sub-stoichiometric ribosomal remodeling (47,83). These specific non-random changes in ribosome remodeling across eukaryotes might lead to specialized ribosomes with specific features needed during a certain type of stress response (47,93–95). A number of RPs showed significant changes in abundance upon MAMP signaling in our study. It is interesting that specific paralogs seem to take over during stress. Martinez-Seidel *et al.* (47) showed that in cold exposed *Arabidopsis*

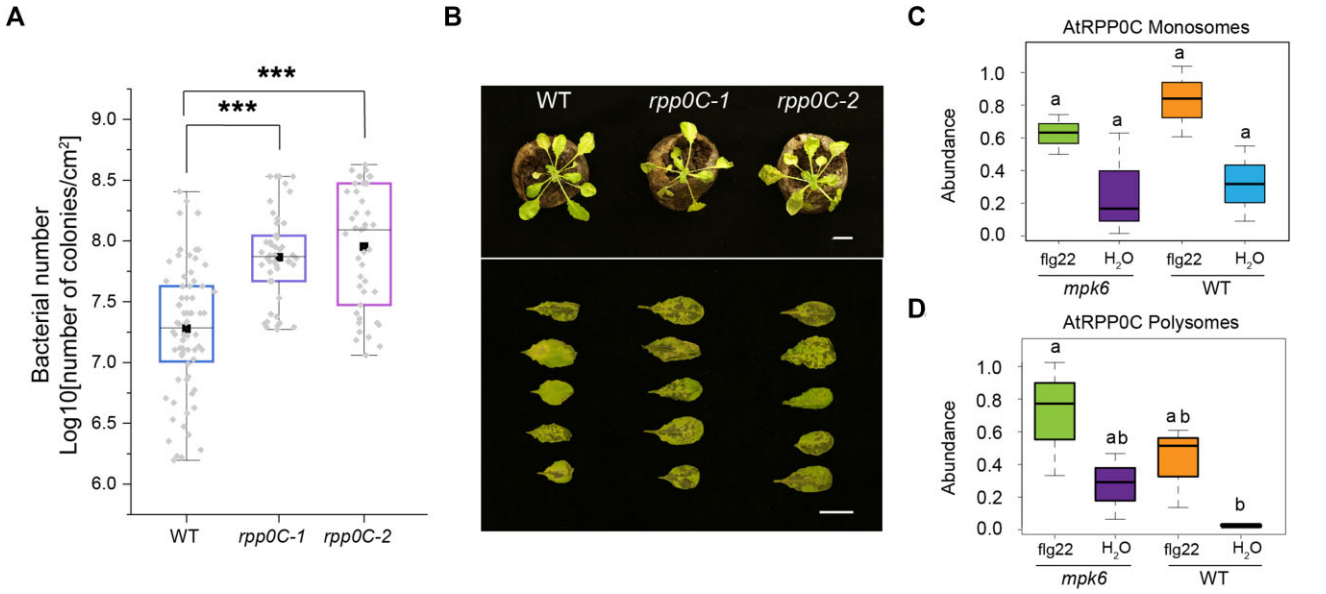

Figure 8. *A. thaliana* mutant *rpp0C-1 and -2* are more resistant towards *Pst* DC3000 than WT. (**A**) *Pst* DC3000 bacterial growth was evaluated at 2 dpi. *Pst* DC3000 pathogen assay results are an average of three biological replicates each consisting of *x* leaf discs ($n = x$). Asterisks indicate significant differences by t.test at $P \leq 0.05$. (**B**) Disease symptoms in WT, *rpp0C-1* and *rpp0C-2* lines. Four-week-old plants were spray-inoculated with *PstDC3000* and pictures were taken 2 days later. Scale bar = 1 cm. (**C**) Tukey HSD plots comparing mean normalized ribosomal protein abundances, identical to those of Figure 5, featuring the change in association of RPP0C with monosomes or (**D**) polysomes of treated and untreated mpk6 and WT plants.

plants, non-random stress-induced ribosomal rearrangements occurs for RP subfamilies with specific spatial localizations. In our study, we obtained similar results confined to the 40S subunit instead of the 60S as happened with cold stress. Furthermore, the ratio between 40S/60S is shifting towards the accumulation of 40S subunit RPs. These findings could point towards an overall reorganization of translation upon stress. For instance, stress induces alternative translation mechanisms such as IRES-dependent translation (2) and alternative translation initiation checkpoints could be used by specialized 40S pre-initiation complexes, which accumulate upon stress and harbor a different RP composition compared to canonical ribosomes. Our hypothesis is supported by the significantly substoichiometric RP localization in the 40S subunit, which we identified to be adjacent to the mRNA and tRNA entry sites. The extent to which 40S subunits with regionally localized r-protein substoichiometry precede the flg22 stimulus and coexist with other 40S populations in the plant cell or if these altered subunits are the outcome of rapid regional ribosome remodeling in response to stress (96) remains an open question.

We also analyzed the function of MPK6 in MAMP-induced ribosomal changes. Disruption of MPK6 function led to additional changes in protein abundance compared to WT plants. In addition to the observed region within the 40S subunit of MAMP-treated WT ribosomes, MAMP treatment of *mpk6* mutant plants resulted in RP changes preferentially localized to the 60S subunit. Specific changes in protein abundance were also identified in monosomes and highlight the importance of MPK6 during the MAMP specific regulation of the 60S subunit. In addition, MPK6 seems to have a strong impact on the ribosomal P-stalk. We found that MPK6 not only affects the abundance of the P-stalk proteins RPP0B/C, RPP1A and RPP3A/B, but also the phosphorylation status of RPP0B/C, RPP1A/C and RPP2A/B/D. These findings are crucial and imply a possible mechanistic explanation of how MPK6 regulates P-stalk function during stress. P0 is a homologue of the prokaryotic L10, whereas P1 and P2 are homologues of prokaryotic L7/L12 (59–62). Besides P0, P1 and P2 (two forms, a and b), plants harbor a third P-protein called P3 (1,32,97). These proteins localize to the conserved lateral protruding stalk of the 60S ribosomal subunit and regulate the translocation process during the elongation cycle of protein synthesis (98). P-proteins do not assemble in the nucleolus on pre-ribosomal complexes but migrate to the cytosol. In addition, P-proteins can occur in multiple copies within a single ribosome which has not been observed for any other RP (99–103). P1 and P2 form dimers in the ribosomal complex, and have unique functions, where P2 cannot bind to the ribosome without P1 (104,105). P1 and P2 play an important function in the regulation of translation elongation, as the enhancement of the interaction between elongation factor eEF2 and the ribosome is dependent on the phosphorylation of both, P1 and P2. However, P2 showed a stronger effect than P1 (66,67). To summarize, P-stalk proteins P1 and P2 seem to regulate translation (106).

In eukaryotes, a main checkpoint of translation is the initiation step, which is accompanied by various protein phosphorylation events (107). Ribosomal subunits and 80S constructs differ from polysomes in their RP-phosphorylation extent. Ribosomal subunits show strong phosphorylation in inactive ribosomes or free ribosomal subunits (108). Our results give new insight into a MAMP-induced phosphorylation regulatory mechanism, which leads to enhanced phosphorylation of P0, but reduced phosphorylation of P1 and P2. In comparison to our results, investigations of anoxia showed that upon stress P1, P2a and P3 get dephosphorylated (106). Other results showed that P1 and P2 dephosphorylation is required to induce an adaptive response to osmotic stress (109). Similarly, our findings would imply a stress specific mechanism which re-

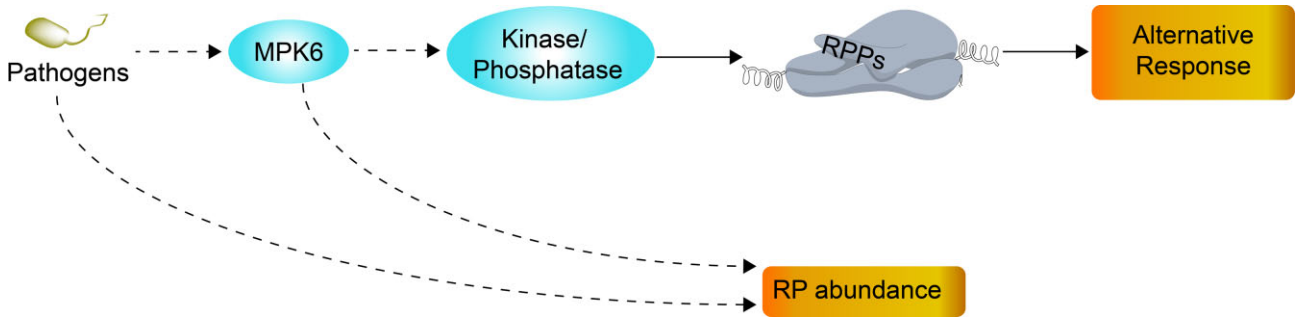

Figure 9. Working model for the role of MPK6 in flg22-induced ribosomal changes. Upon MAMP detection, plants activate MTI via MAPK cascades including the activation of MPK6. MAMP-induced MPK6 activates downstream kinases and phosphatases to alter the phosphorylation status of RPs, including the ribosomal P-stalk. Functional changes in the ribosomal P-stalk might lead to a halt in translation or selective translation of proteins functioning in defense. In addition, MAMP signaling induces changes in RP abundances in an MPK6-dependent and independent manner.

quires P1 and P2 dephosphorylation. In this sense, mutations of serine residues in yeast P1 result in mutants that are less sensitive to osmotic stress, confirming that P1 is necessary for an adaptive stress response (109). Moreover, dephosphorylation of P2 in rats reduces translational activity (67). In *Saccharomyces cerevisiae*, the phosphorylation degree of L7/L12 proteins (homolog of RPP1/2) (110) and of human uL10 (P0 homolog) regulate the affinity of these P-proteins to associate with ribosomes (101). In addition, variations of ribosome-bound abundances of P-proteins lead to differential translation of certain mRNAs (111). Our work supports this idea also genetically by showing that loss of RPP0 protein leads to higher susceptibility of the bacterial pathogen *Pseudomonas syringae* DC3000. Overall, all those findings support the idea that MAMP signaling induced changes in phosphorylation of P-proteins are crucial for plant immunity.

Our study identified MPK6-dependent P-protein phosphorylation events in the C-terminal regions of P0, P1 and P2. All three P-proteins have structurally similar C-termini (112) and C-terminal phosphorylation for acidic plant P-proteins was suggested to influence gene expression upon external stimuli (113). These results suggest that MAMP-triggered MAPK signaling also contributes to defense gene expression via translational regulation. Finally, Briggs & Dinman (27) postulated a question for future investigations: can changes in ribosomal heterogeneity occur in already constituted ribosomes? Our work shows that compositional changes within actively translating polysomes do exist and can be observed already within minutes after stimulus application. Because the RPP phosphorylation sites do not correspond to MAPKs target sites, we propose that MAMP-induced changes in RP phosphorylation are regulated via MPK6-dependent downstream kinases and phosphatases (Figure 9) and further investigations of ribosomal complexes should help to better understand plant innate immunity responses.

Data availability

The mass spectrometry proteomics data have been deposited to the ProteomeXchange Consortium via the PRIDE partner repository with the dataset identifier PXD029502.

Supplementary data

Supplementary Data are available at NAR Online.

Acknowledgements

We would like to thank the KAUST Bioscience Corelabs for technical assistance for proteomics analysis and all members of the Hirt lab.

Author contributions: A.S., N.R. and H.H. designed the study. A.S., F.M.S., N.R., D.G. and J.B. performed the experimental work. A.S., F.M.S., H.A., J.G.K. and N.R. performed *in silico* analysis and analyzed data. A.S., F.M.S., H.H. and N.R. wrote the paper. All authors read and approved the manuscript.

Funding

King Abdullah University of Science and Technology (KAUST) [BAS/1/1062-01-01 to H.H.]. Funding for open access charge: KAUST.

Conflict of interest statement

None declared.

References

1. Barakat,A., Szick-Miranda,K., Chang,I.-F., Guyot,R., Blanc,G., Cooke,R., Delseny,M. and Bailey-Serres,J. (2001) The organization of cytoplasmic ribosomal protein genes in the Arabidopsis fenome. *Plant Physiol.*, **127**, 398–415.
2. Merchante,C., Stepanova,A.N. and Alonso,J.M. (2017) Translation regulation in plants: an interesting past, an exciting present and a promising future. *Plant J.*, **90**, 628–653.
3. Doudna,J.A. and Rath,V.L. (2002) Structure and function of the eukaryotic ribosome: the next frontier. *Cell*, **109**, 153–156.
4. Culver,G.M. (2003) Assembly of the 30S ribosomal subunit. *Biopolymers*, **68**, 234–249.
5. Williamson,J.R. (2003) After the ribosome structures: how are the subunits assembled?*RNA*, **9**, 165–167.
6. Warner,J.R. and McIntosh,K.B. (2009) How common are extraribosomal functions of ribosomal proteins?*Mol. Cell*, **34**, 3–11.
7. Xiong,W., Lan,T. and Mo,B. (2021) Extraribosomal functions of cytosolic ribosomal proteins in plants. *Front. Plant Sci.*, **12**, 607157.
8. Xue,S. and Barna,M. (2012) Specialized ribosomes: a new frontier in gene regulation and organismal biology. *Nat. Rev. Mol. Cell Biol.*, **13**, 355–369.
9. Martinez-Seidel,F., Beine-Golovchuk,O., Hsieh,Y.-C. and Kopka,J. (2020) Systematic review of plant ribosome heterogeneity and specialization. *Front. Plant Sci.*, **11**, 948.

10. Appels,R., Wang,P. and Islam,S. (2021) Integrating wheat nucleolus structure and function: variation in the wheat ribosomal RNA and protein genes. *Front. Plant Sci.*, **12**, 686586.
11. Shrestha,V., Yobi,A., Slaten,M.L., Chan,Y.O., Holden,S., Gyawali,A., Flint-Garcia,S., Lipka,A.E. and Angelovici,R. (2022) Multiomics approach reveals a role of translational machinery in shaping maize kernel amino acid composition. *Plant Physiol.*, **188**, 111–133.
12. Hetti-Arachchilage,M., Challa,G.S. and Marshall-Colón,A. (2021) Rewiring network plasticity to improve crops. *Plant Breed. Rev.*, **45**, 143–183.
13. Fleischer,T.C., Weaver,C.M., McAfee,K.J., Jennings,J.L. and Link,A.J. (2006) Systematic identification and functional screens of uncharacterized proteins associated with eukaryotic ribosomal complexes. *Genes Dev.*, **20**, 1294–1307.
14. Cheong,B.E., Beine-Golovchuk,O., Gorka,M., Ho,W.W.H., Martinez-Seidel,F., Firmino,A.A.P., Skirycz,A., Roessner,U. and Kopka,J. (2021) Arabidopsis REI-LIKE proteins activate ribosome biogenesis during cold acclimation. *Sci. Rep.*, **11**, 2410.
15. Norris,K., Hopes,T. and Aspden,J.L. (2021) Ribosome heterogeneity and specialization in development. *Wiley Interdiscip. Rev. RNA*, **12**, e1644.
16. Ramagopal,S. (1990) Induction of cell-specific ribosomal proteins in aggregation-competent nonmorphogenetic *Dictyostelium discoideum*. *Biochem. Cell. Biol.*, **68**, 1281–1287.
17. Ramagopal,S. and Ennis,H.L. (1981) Regulation of synthesis of cell-specific ribosomal proteins during differentiation of Dictyostelium discoideum. *Proc. Natl. Acad. Sci. U.S.A.*, **78**, 3083–3087.
18. Koyama,K., Wada,A., Maki,Y. and Tanaka,A. (1996) Changes in the protein composition of cytoplasmic ribsomes during the greening of etiolated barley leaves. *Physiol. Plant.*, **96**, 85–90.
19. Weijers,D., Franke-van Dijk,M., Vencken,R.J., Quint,A., Hooykaas,P. and Offringa,R. (2001) An Arabidopsis Minute-like phenotype caused by a semi-dominant mutation in a RIBOSOMAL PROTEIN S5 gene. *Development*, **128**, 4289–4299.
20. Falcone Ferreyra,M.L., Pezza,A., Biarc,J., Burlingame,A.L. and Casati,P. (2010) Plant L10 ribosomal proteins have different roles during development and translation under ultraviolet-B stress. *Plant Physiol.*, **153**, 1878–1894.
21. Whittle,C.A. and Krochko,J.E. (2009) Transcript profiling provides evidence of functional divergence and expression networks among ribosomal protein gene paralogs in Brassica napus. *Plant Cell*, **21**, 2203–2219.
22. Horos,R., Ijspeert,H., Pospisilova,D., Sendtner,R., Andrieu-Soler,C., Taskesen,E., Nieradka,A., Cmejla,R., Sendtner,M., Touw,I.P., *et al.* (2012) Ribosomal deficiencies in Diamond-Blackfan anemia impair translation of transcripts essential for differentiation of murine and human erythroblasts. *Blood*, **119**, 262–272.
23. Zhang,Y. and Lu,H. (2009) Signaling to p53: ribosomal proteins find their way. *Cancer Cell*, **16**, 369–377.
24. Byrne,M.E. (2009) A role for the ribosome in development. *Trends Plant Sci.*, **14**, 512–519.
25. Szakonyi,D. and Byrne,M.E. (2011) Ribosomal protein L27a is required for growth and patterning in *Arabidopsis thaliana*. *Plant J.*, **65**, 269–281.
26. Nishimura,T., Wada,T., Yamamoto,K.T. and Okada,K. (2005) The *Arabidopsis* STV1 protein, responsible for translation reinitiation, is required for auxin-mediated gynoecium patterning. *Plant Cell*, **17**, 2940–2953.
27. Briggs,J.W. and Dinman,J.D. (2017) Subtractional heterogeneity: a crucial step toward defining specialized ribosomes. *Mol. Cell*, **67**, 3–4.
28. Donovan,J. and Copeland,P.R. (2010) Threading the needle: getting selenocysteine into proteins. *Antioxid. Redox. Signal.*, **12**, 881–892.
29. Walsh,C.T., Garneau-Tsodikova,S. and Gatto,G.J. Jr. (2005) Protein posttranslational modifications: the chemistry of proteome diversifications. *Angew. Chem. Int. Ed. Engl.*, **44**, 7342–7372.
30. Beltran-Pena,E., Aguilar,R., Ortiz-Lopez,A., Dinkova,T.D. and de Jimenez,E.S. (2002) Auxin stimulates S6 ribosomal protein phosphorylation in maize thereby affecting protein synthesis regulation. *Physiol. Plant.*, **115**, 291–297.
31. Boex-Fontvieille,E., Daventure,M., Jossier,M., Zivy,M., Hodges,M. and Tcherkez,G. (2013) Photosynthetic control of Arabidopsis leaf cytoplasmic translation initiation by protein phosphorylation. *PLoS One*, **8**, e70692.
32. Chang,I.-F., Szick-Miranda,K., Pan,S. and Bailey-Serres,J. (2005) Proteomic characterization of evolutionarily conserved and variable proteins of Arabidopsis cytosolic ribosomes. *Plant Physiol.*, **137**, 848–862.
33. Khandal,D., Samol,I., Buhr,F., Pollmann,S., Schmidt,H., Clemens,S., Reinbothe,S. and Reinbothe,C. (2009) Singlet oxygen-dependent translational control in the tigrina-d.12mutant of barley. *Proc. Natl. Acad. Sci. U.S.A.*, **106**, 13112–13117.
34. Muench,D.G., Zhang,C. and Dahodwala,M. (2012) Control of cytoplasmic translation in plants. *Wires Rna*, **3**, 178–194.
35. Turck,F., Zilbermann,F., Kozma,S.C., Thomas,G. and Nagy,F. (2004) Phytohormones participate in an S6 kinase signal transduction pathway in Arabidopsis. *Plant Physiol.*, **134**, 1527–1535.
36. Turkina,M.V., Klang Årstrand,H. and Vener,A.V. (2011) Differential phosphorylation of ribosomal proteins in *Arabidopsis thaliana* plants during day and night. *PLoS One*, **6**, e29307.
37. Williams,A.J., Werner-Fraczek,J., Chang,I.-F. and Bailey-Serres,J. (2003) Regulated phosphorylation of 40S ribosomal protein S6 in root tips of maize. *Plant Physiol.*, **132**, 2086–2097.
38. Williamson,N.A., Raliegh,J., Morrice,N.A. and Wettenhall,R.E. (1997) Post-translational processing of rat ribosomal proteins. Ubiquitous methylation of Lys22 within the zinc-finger motif of RL40 (carboxy-terminal extension protein 52) and tissue-specific methylation of Lys4 in RL29. *Eur. J. Biochem.*, **246**, 786–793.
39. Bailey-Serres,J. and Freeling,M. (1990) Hypoxic stress-induced changes in ribosomes of maize seedling roots. *Plant Physiol.*, **94**, 1237.
40. Zhang,Y., Shi,Y., Zhao,L., Wei,F., Feng,Z. and Feng,H. (2019) Phosphoproteomics profiling of cotton (*Gossypium hirsutum* L.) roots in response to *Verticillium dahliae* inoculation. *ACS Omega*, **4**, 18434–18443.
41. Krieg,J., Hofsteenge,J. and Thomas,G. (1988) Identification of the 40 S ribosomal protein S6 phosphorylation sites induced by cycloheximide. *J. Biol. Chem.*, **263**, 11473–11477.
42. Branco-Price,C., Kaiser,K.A., Jang,C.J.H., Larive,C.K. and Bailey-Serres,J. (2008) Selective mRNA translation coordinates energetic and metabolic adjustments to cellular oxygen deprivation and reoxygenation in *Arabidopsis thaliana*. *Plant J.*, **56**, 743–755.
43. Gamm,M., Peviani,A., Honsel,A., Snel,B., Smeekens,S. and Hanson,J. (2014) Increased sucrose levels mediate selective mRNA translation in Arabidopsis. *BMC Plant Biol.*, **14**, 306.
44. Hummel,M., Cordewener,J.H., de Groot,J.C., Smeekens,S., America,A.H. and Hanson,J. (2012) Dynamic protein composition of *Arabidopsis thaliana* cytosolic ribosomes in response to sucrose feeding as revealed by label free MSE proteomics. *Proteomics*, **12**, 1024–1038.
45. Juntawong,P., Girke,T., Bazin,J. and Bailey-Serres,J. (2014) Translational dynamics revealed by genome-wide profiling of ribosome footprints in Arabidopsis. *Proc. Natl. Acad. Sci. U.S.A.*, **111**, E203–E212.
46. Pal,S.K., Liput,M., Piques,M., Ishihara,H., Obata,T., Martins,M.C., Sulpice,R., van Dongen,J.T., Fernie,A.R., Yadav,U.P., *et al.* (2013) Diurnal changes of polysome loading

track sucrose content in the rosette of wild-type arabidopsis and the starchless pgm mutant. *Plant Physiol.*, **162**, 1246–1265.
47. Martinez-Seidel,F., Beine-Golovchuk,O., Hsieh,Y.C., Eshraky,K.E., Gorka,M., Cheong,B.E., Jimenez-Posada,E.V., Walther,D., Skirycz,A., Roessner,U., *et al.* (2021) Spatially enriched paralog rearrangements argue functionally diverse ribosomes arise during cold acclimation in Arabidopsis. *Int. J. Mol. Sci.*, **22**, 6160.
48. Nagaraj,S., Senthil-Kumar,M., Ramu,V.S., Wang,K. and Mysore,K.S. (2016) Plant ribosomal proteins, RPL12 and RPL19, play a role in nonhost disease resistance against bacterial pathogens. *Front. Plant Sci.*, **6**, 1192–1192.
49. Savary,S., Ficke,A., Aubertot,J.-N. and Hollier,C. (2012) Crop losses due to diseases and their implications for global food production losses and food security. *Food Secur.*, **4**, 519–537.
50. Godfray,H.C.J., Beddington,J.R., Crute,I.R., Haddad,L., Lawrence,D., Muir,J.F., Pretty,J., Robinson,S., Thomas,S.M. and Toulmin,C. (2010) Food security: the challenge of feeding 9 billion people. *Science*, **327**, 812.
51. Gomez-Gomez,L. and Boller,T. (2000) FLS2: an LRR receptor-like kinase involved in the perception of the bacterial elicitor flagellin in Arabidopsis. *Mol. Cell*, **5**, 1003–1011.
52. Nühse,T.S., Bottrill,A.R., Jones,A.M.E. and Peck,S.C. (2007) Quantitative phosphoproteomic analysis of plasma membrane proteins reveals regulatory mechanisms of plant innate immune responses. *Plant J.*, **51**, 931–940.
53. Rayapuram,N., Bonhomme,L., Bigeard,J., Haddadou,K., Przybylski,C., Hirt,H. and Pflieger,D. (2014) Identification of novel PAMP-triggered phosphorylation and dephosphorylation events in Arabidopsis thaliana by quantitative phosphoproteomic analysis. *J. Proteome Res.*, **13**, 2137–2151.
54. Moore,J.W., Loake,G.J. and Spoel,S.H. (2011) Transcription dynamics in plant immunity. *Plant Cell*, **23**, 2809–2820.
55. Feilner,T., Hultschig,C., Lee,J., Meyer,S., Immink,R.G., Koenig,A., Possling,A., Seitz,H., Beveridge,A., Scheel,D., *et al.* (2005) High throughput identification of potential Arabidopsis mitogen-activated protein kinases substrates. *Mol. Cell. Proteomics*, **4**, 1558–1568.
56. Takáč,T., Vadovič,P., Pechan,T., Luptovčiak,I., Šamajová,O. and Šamaj,J. (2016) Comparative proteomic study of Arabidopsis mutants mpk4 and mpk6. *Sci. Rep.*, **6**, 28306.
57. Rayapuram,N., Bigeard,J., Alhoraibi,H., Bonhomme,L., Hesse,A.M., Vinh,J., Hirt,H. and Pflieger,D. (2018) Quantitative phosphoproteomic analysis reveals shared and specific targets of Arabidopsis mitogen-activated protein kinases (MAPKs) MPK3, MPK4, and MPK6. *Mol. Cell. Proteomics*, **17**, 61–80.
58. Wahl,M.C. and Moller,W. (2002) Structure and function of the acidic ribosomal stalk proteins. *Curr. Protein Pept. Sci.*, **3**, 93–106.
59. Santos,C. and Ballesta,J.P. (1995) The highly conserved protein P0 carboxyl end is essential for ribosome activity only in the absence of proteins P1 and P2. *J. Biol. Chem.*, **270**, 20608–20614.
60. Santos,C. and Ballesta,J.P. (1994) Ribosomal protein P0, contrary to phosphoproteins P1 and P2, is required for ribosome activity and *Saccharomyces cerevisiae* viability. *J. Biol. Chem.*, **269**, 15689–15696.
61. Uchiumi,T., Wahba,A.J. and Traut,R.R. (1987) Topography and stoichiometry of acidic proteins in large ribosomal subunits from *Artemia salina* as determined by crosslinking. *Proc. Natl. Acad. Sci. U. S. A.*, **84**, 5580–5584.
62. Uchiumi,T. and Kominami,R. (1992) Direct evidence for interaction of the conserved GTPase domain within 28 S RNA with mammalian ribosomal acidic phosphoproteins and L12. *J. Biol. Chem.*, **267**, 19179–19185.
63. Sánchez-Madrid,F., Reyes,R., Conde,P. and Ballesta,J.P. (1979) Acidic ribosomal proteins from eukaryotic cells. Effect on ribosomal functions. *Eur. J. Biochem.*, **98**, 409–416.
64. MacConnell,W.P. and Kaplan,N.O. (1982) The activity of the acidic phosphoproteins from the 80 S rat liver ribosome. *J. Biol. Chem.*, **257**, 5359–5366.
65. Uchiumi,T., Kikuchi,M., Terao,K., Iwasaki,K. and Ogata,K. (1986) Cross-linking of elongation factor 2 to rat-liver ribosomal proteins by 2-iminothiolane. *Eur. J. Biochem.*, **156**, 37–48.
66. Bargis-Surgey,P., Lavergne,J.P., Gonzalo,P., Vard,C., Filhol-Cochet,O. and Reboud,J.P. (1999) Interaction of elongation factor eEF-2 with ribosomal P proteins. *Eur. J. Biochem.*, **262**, 606–611.
67. Vard,C., Guillot,D., Bargis,P., Lavergne,J.P. and Reboud,J.P. (1997) A specific role for the phosphorylation of mammalian acidic ribosomal protein P2. *J. Biol. Chem.*, **272**, 20259–20262.
68. Möller,W., Slobin,L.I., Amons,R. and Richter,D. (1975) Isolation and characterization of two acidic proteins of 60s ribosomes from Artemia salina cysts. *Proc. Natl. Acad. Sci. U.S.A.*, **72**, 4744.
69. Uchiumi,T., Traut,R.R. and Kominami,R. (1990) Monoclonal antibodies against acidic phosphoproteins P0, P1, and P2 of eukaryotic ribosomes as functional probes. *J. Biol. Chem.*, **265**, 89–95.
70. Nakagami,H., Soukupová,H., Schikora,A., Zárský,V. and Hirt,H. (2006) A Mitogen-activated Protein Kinase Kinase Kinase Mediates Reactive Oxygen Species Homeostasis in Arabidopsis. *J. Biol. Chem.*, **281**, 38697–38704.
71. Mustroph,A., Juntawong,P. and Bailey-Serres,J. In: Belostotsky,D.A. (ed.) *Plant Systems Biology*. Humana Press, Totowa, NJ, pp. 109–126.
72. Rayapuram,N., Jarad,M., Alhoraibi,H.M., Bigeard,J., Abulfaraj,A.A., Völz,R., Mariappan,K.G., Almeida-Trapp,M., Schlöffel,M., Lastrucci,E., *et al.* (2021) Chromatin phosphoproteomics unravels a function for AT-hook motif nuclear localized protein AHL13 in PAMP-triggered immunity. *Proc. Natl. Acad. Sci. USA*, **118**.
73. Team, R.C. (2018) *R: A Language and Environment for Statistical Computing*. R Foundation for Statistical Computing.
74. Firmino,A.A.P., Gorka,M., Graf,A., Skirycz,A., Martinez-Seidel,F., Zander,K., Kopka,J. and Beine-Golovchuk,O. (2020) Separation and paired proteome profiling of plant chloroplast and cytoplasmic ribosomes. *Plants (Basel)*, **9**, 892.
75. Armache,J.-P., Jarasch,A., Anger,A.M., Villa,E., Becker,T., Bhushan,S., Jossinet,F., Habeck,M., Dindar,G., Franckenberg,S., *et al.* (2010) Cryo-EM structure and rRNA model of a translating eukaryotic 80S ribosome at 5.5-Å resolution. *Proc. Natl. Acad. Sci. U.S.A.*, **107**, 19748–19753.
76. Martinez-Seidel,F., Hsieh,Y.C., Walther,D., Kopka,J. and Pereira Firmino,A.A. (2021) ComplexOme-Structural Network Interpreter used to study spatial enrichment in metazoan ribosomes. *BMC Bioinf.*, **22**, 605.
77. Asai,T., Tena,G., Plotnikova,J., Willmann,M.R., Chiu,W.L., Gomez-Gomez,L., Boller,T., Ausubel,F.M. and Sheen,J. (2002) MAP kinase signalling cascade in Arabidopsis innate immunity. *Nature*, **415**, 977–983.
78. Lee,J., Eschen-Lippold,L., Lassowskat,I., Böttcher,C. and Scheel,D. (2015) Cellular reprogramming through mitogen-activated protein kinases. *Front. Plant Sci.*, **6**, 940–940.
79. Xu,J. and Chua,N.H. (2012) Dehydration stress activates Arabidopsis MPK6 to signal DCP1 phosphorylation. *EMBO J.*, **31**, 1975–1984.
80. Roux,M.E., Rasmussen,M.W., Palma,K., Lolle,S., Regué,À.,M., Bethke,G., Glazebrook,J., Zhang,W., Sieburth,L., Larsen,M.R., *et al.* (2015) The mRNA decay factor PAT1 functions in a pathway including MAP kinase 4 and immune receptor SUMM2. *EMBO J.*, **34**, 593–608.
81. Kedersha,N., Stoecklin,G., Ayodele,M., Yacono,P., Lykke-Andersen,J., Fritzler,M.J., Scheuner,D., Kaufman,R.J., Golan,D.E. and Anderson,P. (2005) Stress granules and processing bodies are dynamically linked sites of mRNP remodeling. *J. Cell Biol.*, **169**, 871–884.

82. Berková,V., Kameniarová,M., Ondrisková,V., Berka,M., Menšíková,S., Kopecká,R., Luklová,M., Novák,J., Spíchal,L. and Rashotte,A.M. (2020) Arabidopsis response to Inhibitor of Cytokinin Degradation INCYDE: modulations of cytokinin signaling and plant proteome. *Plants*, **9**, 1563.
83. Martinez-Seidel,F., Suwanchaikasem,P., Nie,S., Leeming,M.G., Pereira Firmino,A.A., Williamson,N.A., Kopka,J., Roessner,U. and Boughton,B.A. (2021) Membrane-enriched proteomics link ribosome accumulation and proteome reprogramming with cold acclimation in barley root meristems. *Front. Plant Sci.*, **12**, 656683.
84. Liu,H.M., Long,C.R., Wang,S.H., Fu,X.M., Zhou,X.Y., Mao,J.M., Yang,H.X., Du,Y.X., Li,J.X., Yue,J.Q., *et al.* (2021) Transcriptome and metabolome comparison of smooth and rough *Citrus limon* L. peels grown on same trees and harvested in different seasons. *Front. Plant Sci.*, **12**, 749803.
85. Moin,M., Saha,A., Bakshi,A., Madhav,M.S. and Kirti,P.B. (2021) Constitutive expression of Ribosomal Protein L6 modulates salt tolerance in rice transgenic plants. *Gene*, **789**, 145670.
86. Kimberlin,A., Holtsclaw,R.E. and Koo,A.J. (2021) Differential regulation of the ribosomal association of mRNA transcripts in an Arabidopsis mutant defective in Jasmonate-dependent wound response. *Front. Plant Sci.*, **12**, 637959.
87. Kokila,S. and Devaraj,V.R. (2021) A comparative study of ESTs induced under drought and salinity stress in Hyacinth bean (*Lablab purpureus*). *Am. J. Plant Sci.*, **12**, 840–857.
88. Fernie,A.R. and Stitt,M. (2012) On the discordance of metabolomics with proteomics and transcriptomics: coping with increasing complexity in logic, chemistry, and network interactions scientific correspondence. *Plant Physiol.*, **158**, 1139–1145.
89. Caplan,J., Padmanabhan,M. and Dinesh-Kumar,S.P. (2008) Plant NB-LRR immune receptors: from recognition to transcriptional reprogramming. *Cell Host Microbe*, **3**, 126–135.
90. Smith,J.E., Mengesha,B., Tang,H., Mengiste,T. and Bluhm,B.H. (2014) Resistance to *Botrytis cinerea* in *Solanum lycopersicoides* involves widespread transcriptional reprogramming. *Bmc Genomics [Electronic Resource]*, **15**, 334.
91. Xu,G., Greene,G.H., Yoo,H., Liu,L., Marqués,J., Motley,J. and Dong,X. (2017) Global translational reprogramming is a fundamental layer of immune regulation in plants. *Nature*, **545**, 487–490.
92. Yoo,H., Greene,G.H., Yuan,M., Xu,G., Burton,D., Liu,L., Marqués,J. and Dong,X. (2020) Translational Regulation of Metabolic Dynamics during Effector-Triggered Immunity. *Mol. Plant*, **13**, 88–98.
93. Bates,C., Hubbard,S.J. and Ashe,M.P. (2018) Ribosomal flavours: an acquired taste for specific mRNAs? *Biochem. Soc. Trans.*, **46**, 1529–1539.
94. Genuth,N.R. and Barna,M. (2018) Heterogeneity and specialized functions of translation machinery: from genes to organisms. *Nat. Rev. Genet.*, **19**, 431–452.
95. Komili,S., Farny,N.G., Roth,F.P. and Silver,P.A. (2007) Functional specificity among ribosomal proteins regulates gene expression. *Cell*, **131**, 557–571.
96. Yang,Y.M. and Karbstein,K. (2022) The chaperone Tsr2 regulates Rps26 release and reincorporation from mature ribosomes to enable a reversible, ribosome-mediated response to stress. *Sci. Adv.*, **8**, eabl4386.
97. Carroll,A.J. (2013) The Arabidopsis cytosolic ribosomal proteome: from form to function. *Front. Plant Sci.*, **4**, 32.
98. Shankweller,G.W., Scheinman,A.O. and Lake,J.A. (1991) The ribosome: structure, function and evolution. In: Hill,W.E., Moore,P.B., Dahlberg,A., Schlessinger,D., Garrett,R.A. and Warner,J.R. (eds.) *Trends in Cell Biology*. American Society for Microbiology, Vol. **1**, p. 75.
99. van Agthoven,A., Kriek,J., Amons,R. and Möller,W. (1978) Isolation and characterization of the acidic phosphoproteins of 60-S ribosomes from Artemia salina and rat liver. *Eur. J. Biochem.*, **91**, 553–565.
100. Zinker,S. (1980) P5/P5' the acidic ribosomal phosphoproteins from *Saccharomyces cerevisiae*. *Biochim. Biophys. Acta*, **606**, 76–82.
101. Sánchez-Madrid,F., Vidales,F.J. and Ballesta,J.P. (1981) Effect of phosphorylation on the affinity of acidic proteins from *Saccharomyces cerevisiae* for the ribosomes. *Eur. J. Biochem.*, **114**, 609–613.
102. Elkon,K., Skelly,S., Parnassa,A., Moller,W., Danho,W., Weissbach,H. and Brot,N. (1986) Identification and chemical synthesis of a ribosomal protein antigenic determinant in systemic lupus erythematosus. *Proc. Natl. Acad. Sci. U.S.A.*, **83**, 7419–7423.
103. Tsurugi,K. and Ogata,K. (1985) Evidence for the exchangeability of acidic ribosomal proteins on cytoplasmic ribosomes in regenerating rat liver. *J. Biochem.*, **98**, 1427–1431.
104. Remacha,M., Santos,C., Bermejo,B., Naranda,T. and Ballesta,J.P. (1992) Stable binding of the eukaryotic acidic phosphoproteins to the ribosome is not an absolute requirement for in vivo protein synthesis. *J. Biol. Chem.*, **267**, 12061–12067.
105. Zurdo,J., Parada,P., van den Berg,A., Nusspaumer,G., Jimenez-Diaz,A., Remacha,M. and Ballesta,J.P. (2000) Assembly of Saccharomyces cerevisiae ribosomal stalk: binding of P1 proteins is required for the interaction of P2 proteins. *Biochemistry*, **39**, 8929–8934.
106. Szick-Miranda,K. and Bailey-Serres,J. (2001) Regulated heterogeneity in 12-kDa P-protein phosphorylation and composition of ribosomes in maize (*Zea mays* L.). *J. Biol. Chem.*, **276**, 10921–10928.
107. Jackson,R.J., Hellen,C.U.T. and Pestova,T.V. (2010) The mechanism of eukaryotic translation initiation and principles of its regulation. *Nat. Rev. Mol. Cell Biol.*, **11**, 113.
108. Imami,K., Milek,M., Bogdanow,B., Yasuda,T., Kastelic,N., Zauber,H., Ishihama,Y., Landthaler,M. and Selbach,M. (2018) Phosphorylation of the ribosomal protein RPL12/uL11 affects translation during mitosis. *Mol. Cell*, **72**, 84–98.
109. Zambrano,R., Briones,E., Remacha,M. and Ballesta,J.P. (1997) Phosphorylation of the acidic ribosomal P proteins in Saccharomyces cerevisiae: a reappraisal. *Biochemistry*, **36**, 14439–14446.
110. Wool,I.G., Chan,Y.L., Glück,A. and Suzuki,K. (1991) The primary structure of rat ribosomal proteins P0, P1, and P2 and a proposal for a uniform nomenclature for mammalian and yeast ribosomal proteins. *Biochimie*, **73**, 861–870.
111. Remacha,M., Jimenez-Diaz,A., Bermejo,B., Rodriguez-Gabriel,M.A., Guarinos,E. and Ballesta,J.P. (1995) Ribosomal acidic phosphoproteins P1 and P2 are not required for cell viability but regulate the pattern of protein expression in *Saccharomyces cerevisiae*. *Mol. Cell. Biol.*, **15**, 4754–4762.
112. Ballesta,J.P.G. and Remacha,M. (1996) In: Cohn,W.E. and Moldave,K. (eds.) *Progress in Nucleic Acid Research and Molecular Biology*. Academic Press, San Diego, Vol. **55**, pp. 157–193.
113. Reiland,S., Messerli,G., Baerenfaller,K., Gerrits,B., Endler,A., Grossmann,J., Gruissem,W. and Baginsky,S. (2009) Large-scale Arabidopsis phosphoproteome profiling reveals novel chloroplast kinase substrates and phosphorylation networks. *Plant Physiol.*, **150**, 889.
114. Armache,J.-P., Jarasch,A., Anger,A.M., Villa,E., Becker,T., Bhushan,S., Jossinet,F., Habeck,M., Dindar,G., Franckenberg,S., *et al.* (2010) Localization of eukaryote-specific ribosomal proteins in a 5.5-Å cryo-EM map of the 80S eukaryotic ribosome. *Proc. Natl. Acad. Sci. U.S.A.*, **107**, 19754.

Received: June 24, 2023. **Revised:** September 14, 2023. **Editorial Decision:** September 19, 2023. **Accepted:** September 20, 2023